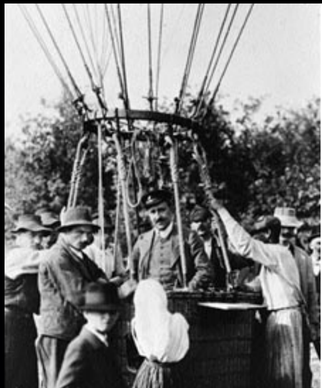

100 years

NEW DEVELOPMENTS IN ASTROPHYSICS OF COSMIC RAYS

IGOR V MOSKALENKO – STANFORD

$\bar{d}$19 • UCLA • Mar. 27 – 29, 2019

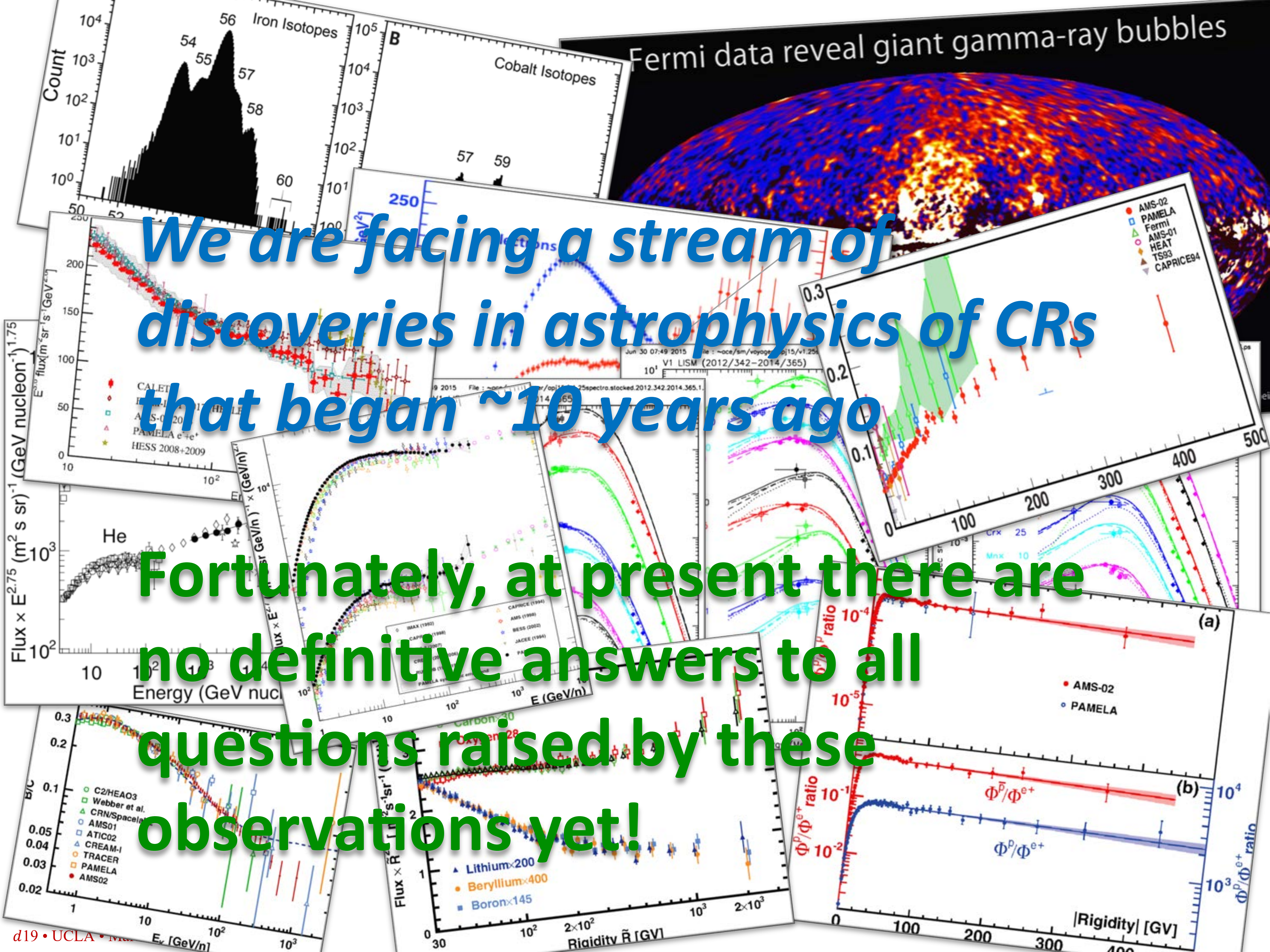

We are facing a stream of discoveries in astrophysics of CRs that began ~10 years ago

Fortunately, at present there are no definitive answers to all questions raised by these observations yet!

Timeline of γ-ray, CR, and particle experiments

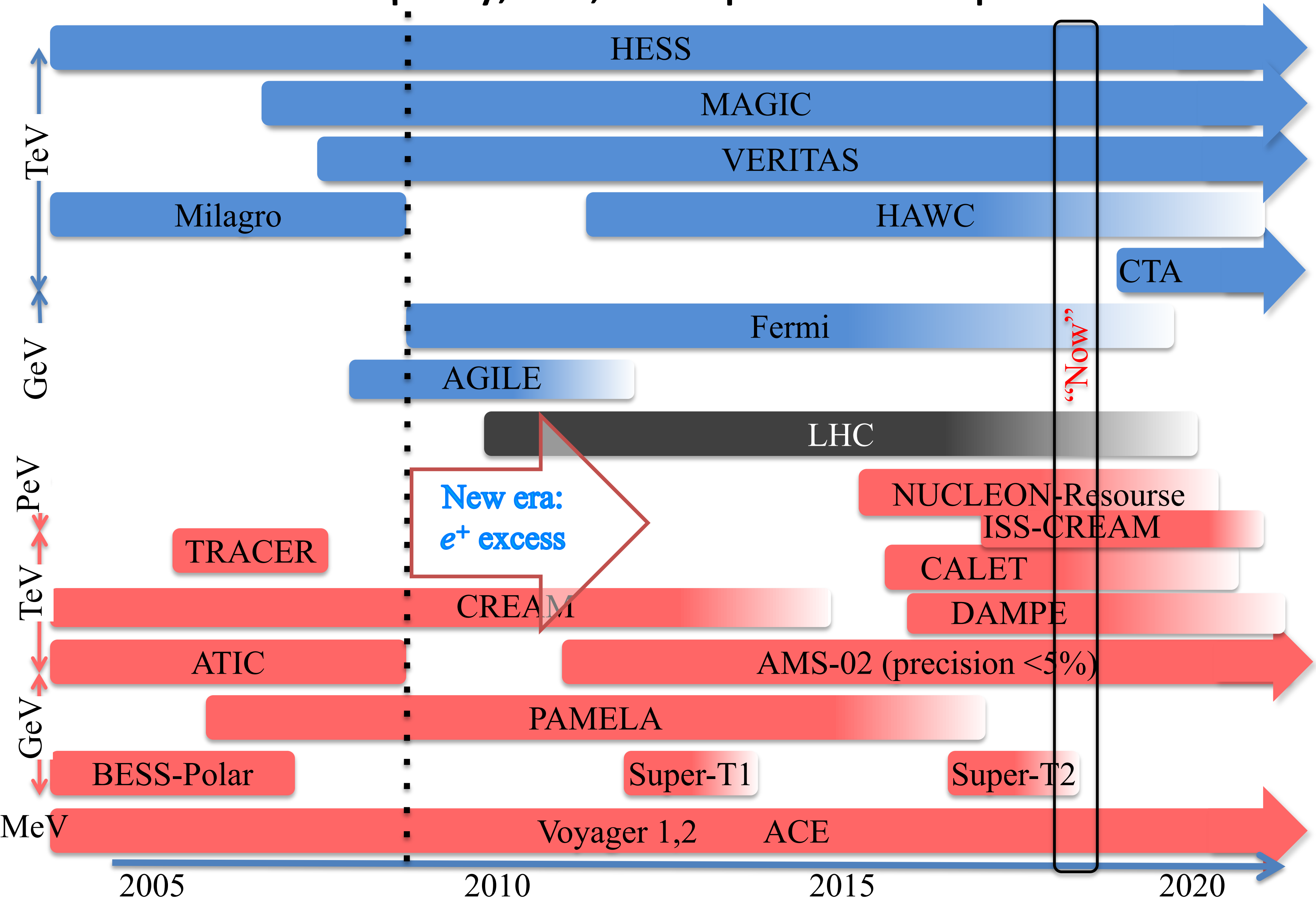

Crab nebula – SN 1054

New discoveries in Astrophysics of CRs lead us to:

- ✧ Improve our understanding of the conventional astrophysical backgrounds
- ✧ Provide new insights into conventional processes in astrophysical objects or between them (interstellar/intergalactic medium)
- ✧ Potentially uncover signatures of new/exotic physics that we still have to understand
- ✧ Or to better understanding of the instruments

"Guest star" – in Chinese records

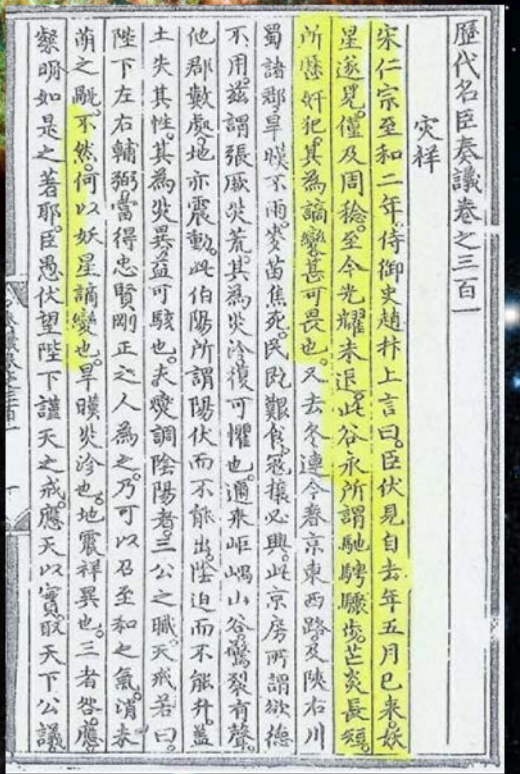

歷代名臣奏議卷之三百一
災祥
宋仁宗至和二年侍御史趙抃上言曰臣伏見自去年五月已來妖
星遂見僅及周稔至今光耀未退此谷永所謂馳騁驟歷芒炎長短
所歷奸犯其為讁變甚可畏也又去冬連今春京東西路及陝右川
蜀諸郡旱暵不雨麥苗焦死民既艱食寇攘必興此京房所謂欲德
不用茲謂張厥災荒其為災沴復可懼也迺來岷峨山谷驚裂有聲
他郡數處地亦震動此伯陽所謂陽伏而不能出陰迫而不能升蓋
土失其性其為災異益可駭也夫燮調陰陽者三公之職天戒若曰
陛下左右輔弼當得忠賢剛正之人為之乃可以召至和之氣消去
萌之厲不然何以妖星讁變也旱暵災沴也地震祥異也三者咎應
粲明如是之著耶臣愚伏望陛下謹天之戒應天以實取天下公議

EGRET GeV excess

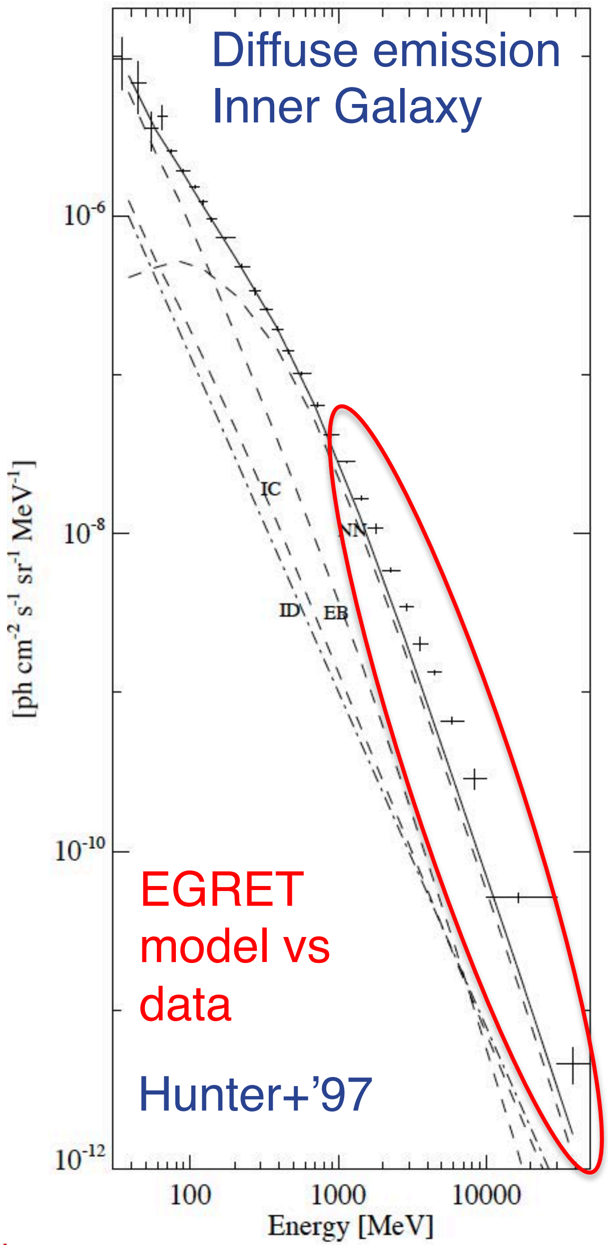

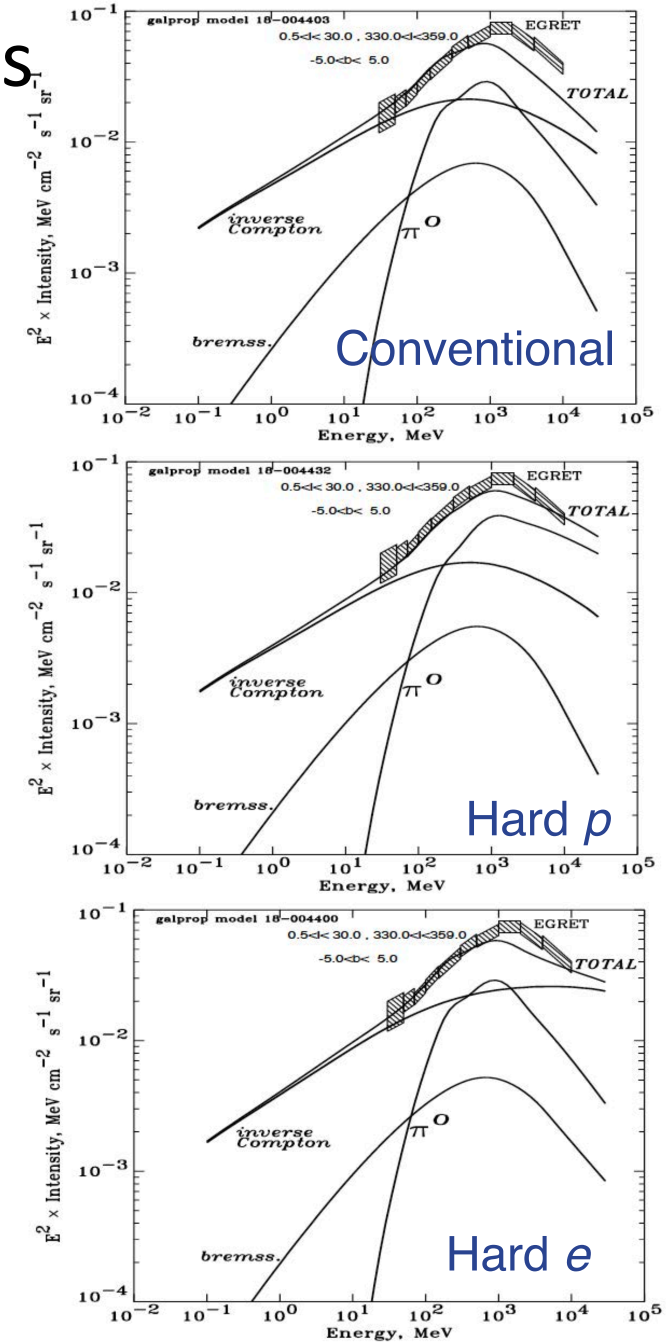

"Diffuse galactic gamma rays, cosmic-ray nucleons and antiprotons"

IM, Strong, Reimer'98

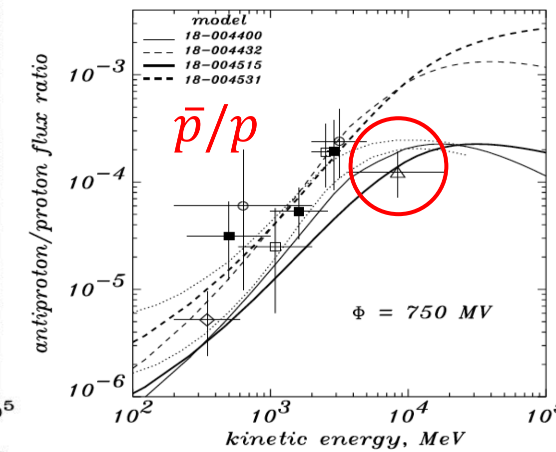

- ✧ Antiproton test of the nucleon spectrum
- ✧ A single $\bar{p}/p$ data point was used to put a restriction on the hard spectrum of CR nucleons

DM discovery (de Boer+)

EGRET diffuse emission

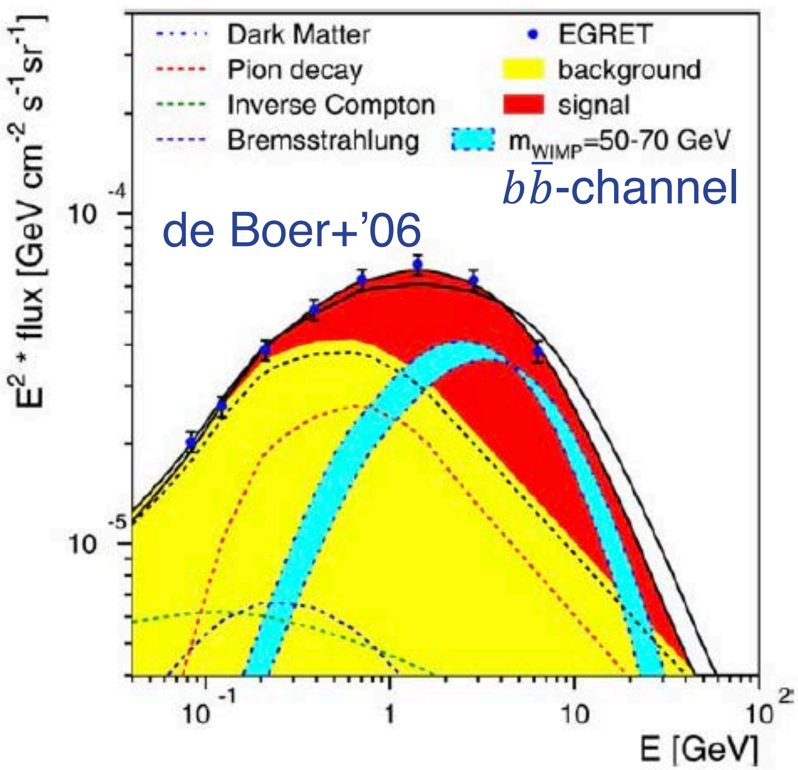

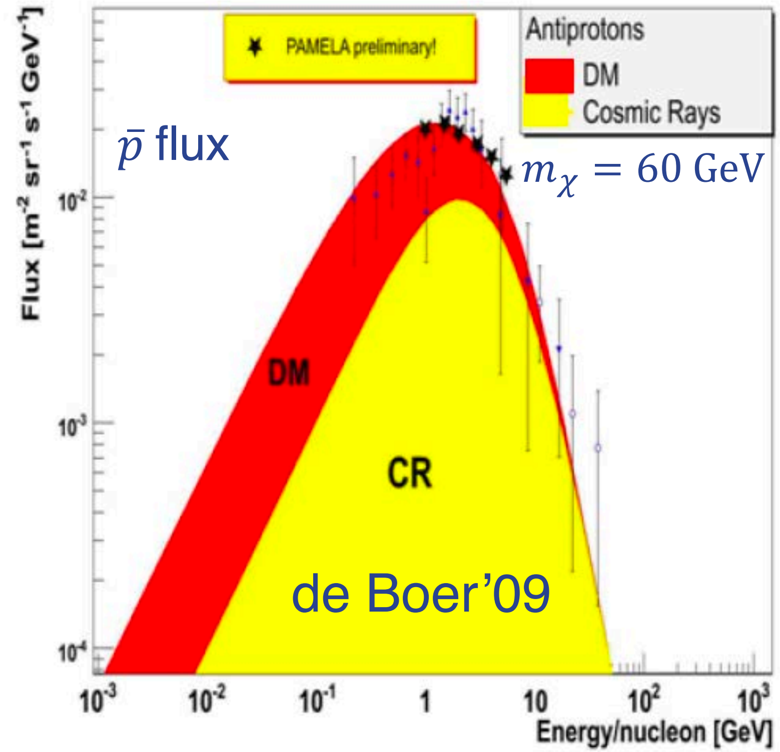

- The DM discovery was claimed by de Boer et al. in numerous papers: consistency between excess in diffuse γ-rays and $\bar{p}$
- All possible EGRET systematics was neglected, even though at some point it has become clear that the GeV excess was likely instrumental (IM+'07)

Fermi-LAT observations

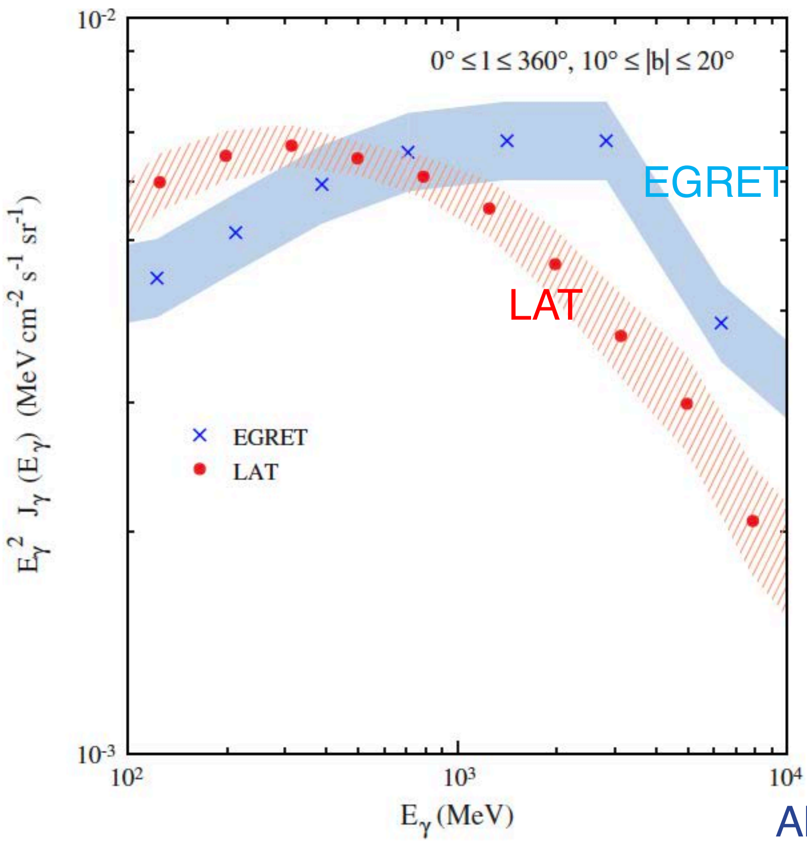

Abdo+'09

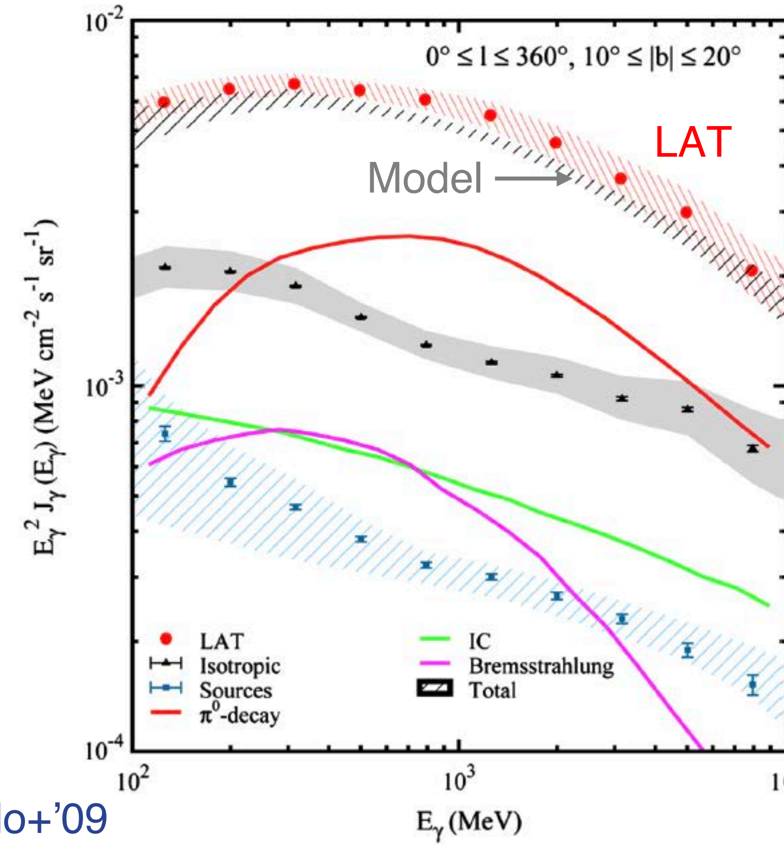

- ✧ LAT measurements of the spectrum of the diffuse emission clearly show that the EGRET GEV excess is instrumental
- ✧ The spectrum of the diffuse emission by LAT is in a good agreement with prediction of the conventional model

AMS-01: A 50 GeV bump in the proton spectrum

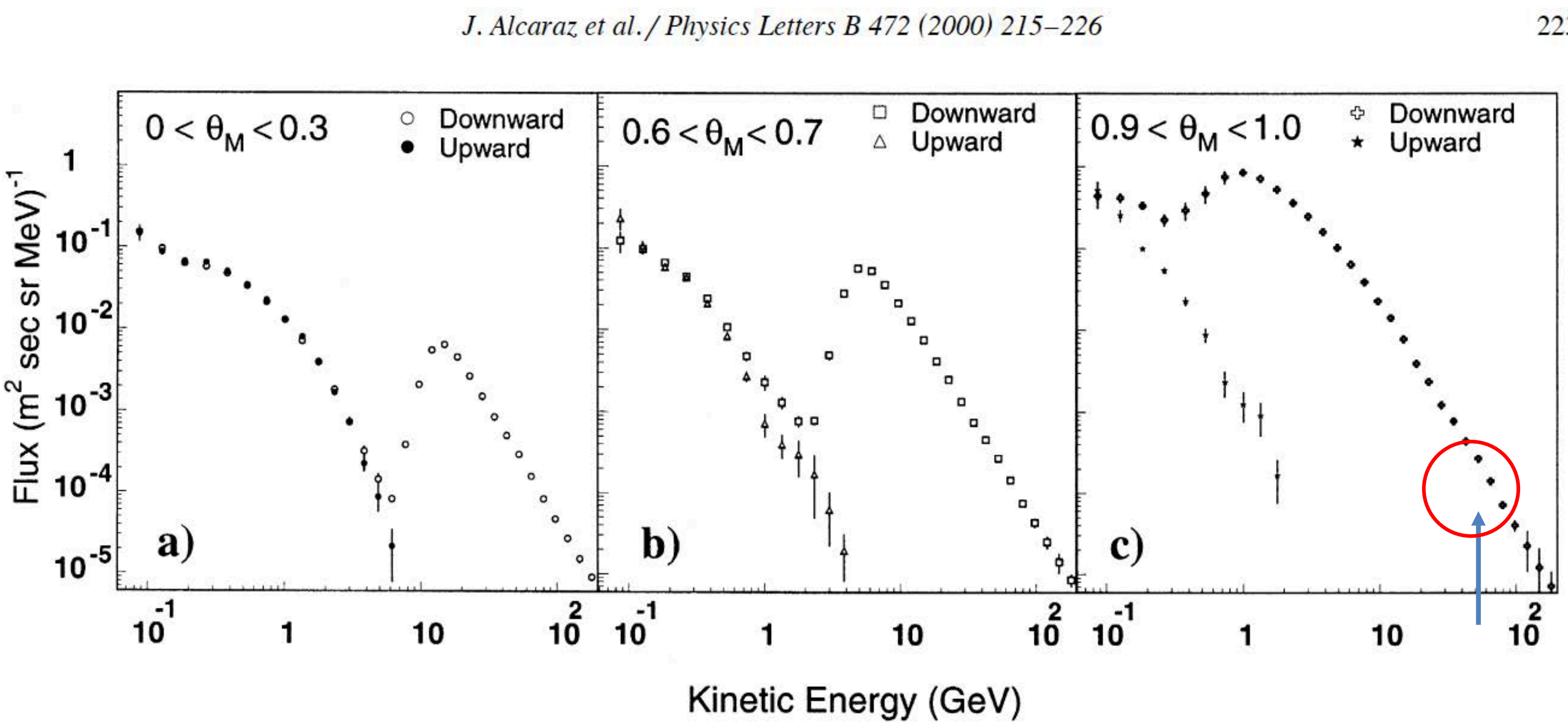

✧ Hardly seen in the log-log scale, but some people noticed it 😃 including myself

Interpretation of 50 GeV excess

Fine structure in the energy spectrum of cosmic ray protons at 50 GeV?
A.D. Erlykin, S.J. Fatemi, A. W. Wolfendale
Physics Letters B 482 (2000) 337-342

- ✧ Excess was found in all available CR proton data!
- ✧ Their interpretation:
  - – Technical factors (unlikely)
  - – Protons from exotic processes
  - – SNR effects
  - – Heliospheric shock
- ✧ This bump disappeared in a follow up paper by AMS-01 (2000PhLB..490…27A)

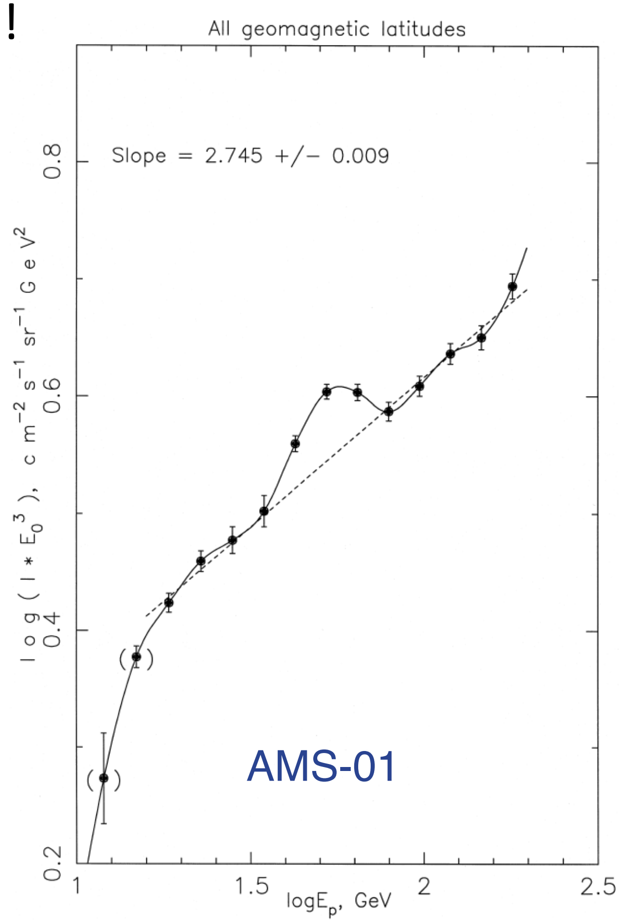

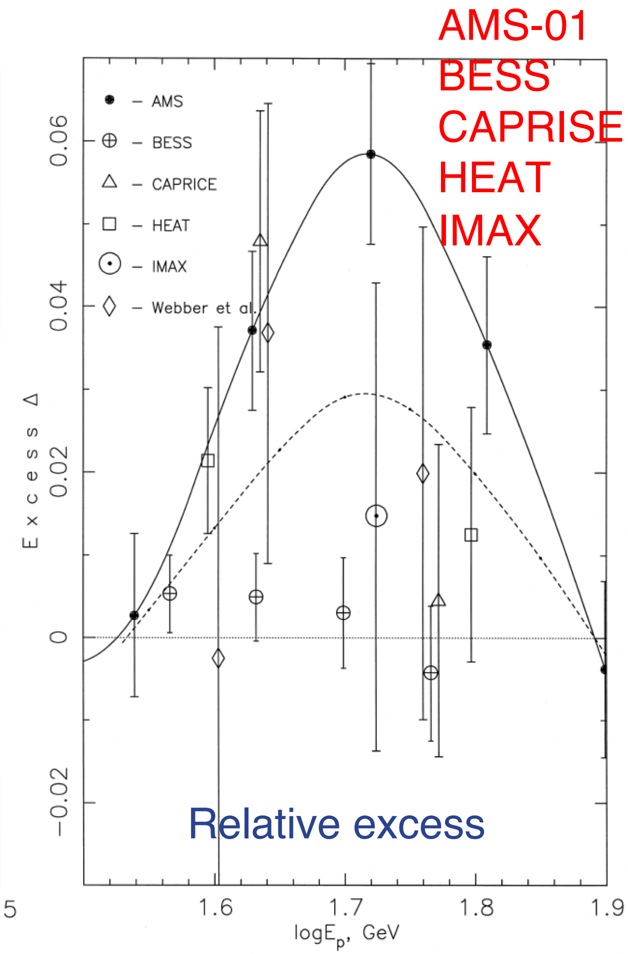

ATIC electron excess 300-800 GeV (Chang+'08)

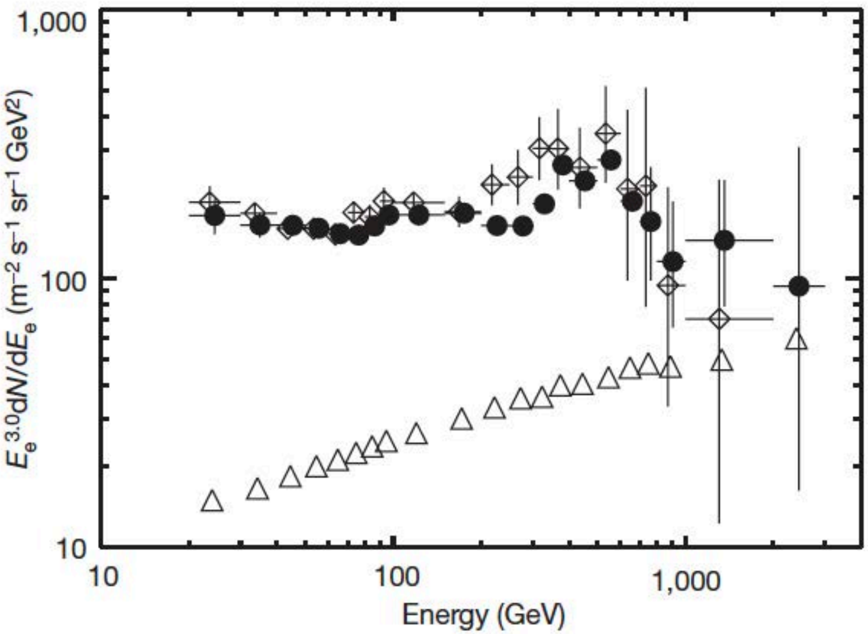

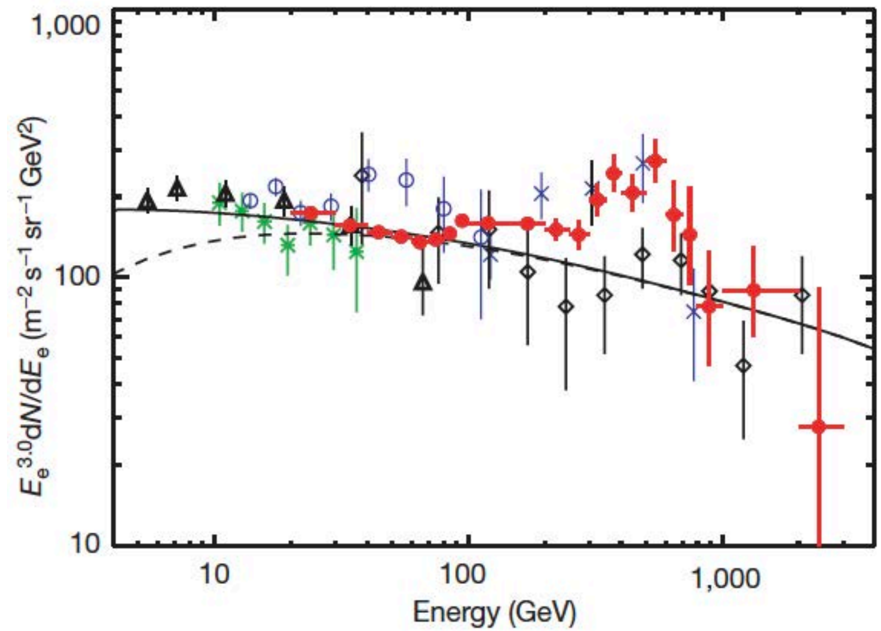

- ✧ ATIC-1 and ATIC-2 show consistent results
- ✧ A hint of the excess is seen in data of other experiments (PPB-BETS, emulsion chambers)
- ✧ Local CR *e* source
- ✧ Annihilation of Kaluza-Klein particles

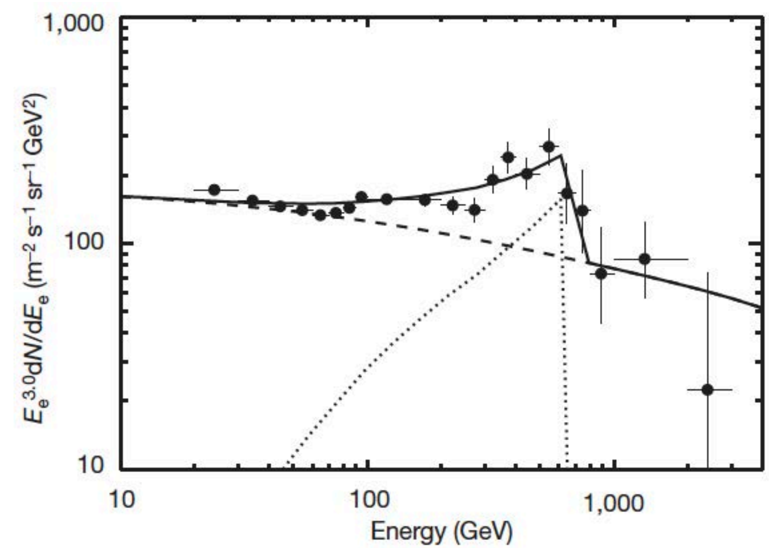

All-electron measurements

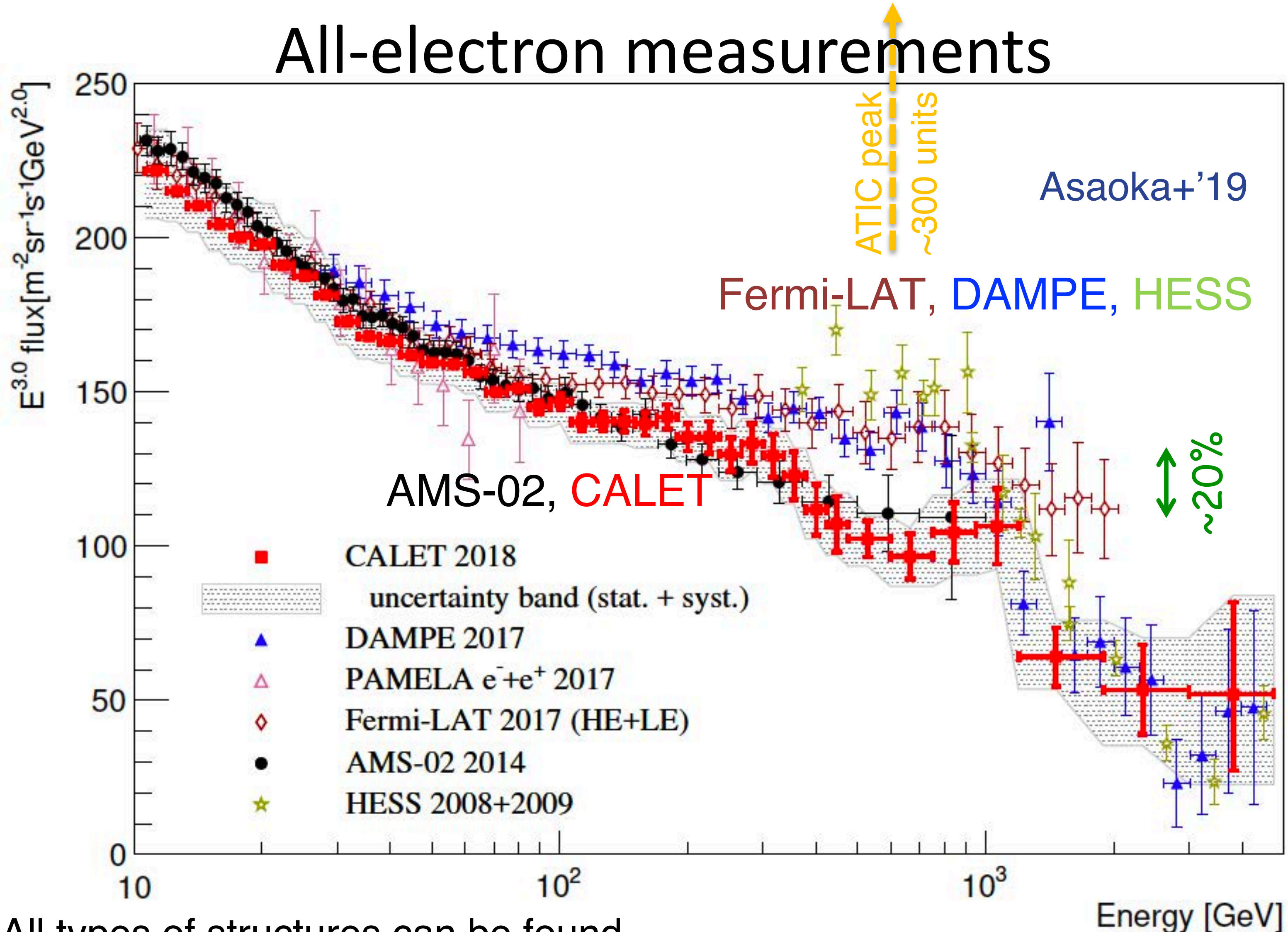

- ✧ All types of structures can be found
- ✧ Results by pairs of instruments (AMS-02 & CALET) and (Fermi-LAT & DAMPE) confirm each other, but look quite different from another pair with high significance!

GeV excess in antiprotons

- ✧ The reacceleration model worked fairly well for all CR data except $\bar{p}$
- ✧ It underpredicted the $\bar{p}$ flux compared to BESS data by ~40%
- ✧ A significant effort was made to find a model that would be able to reproduce the observed $\bar{p}$ flux

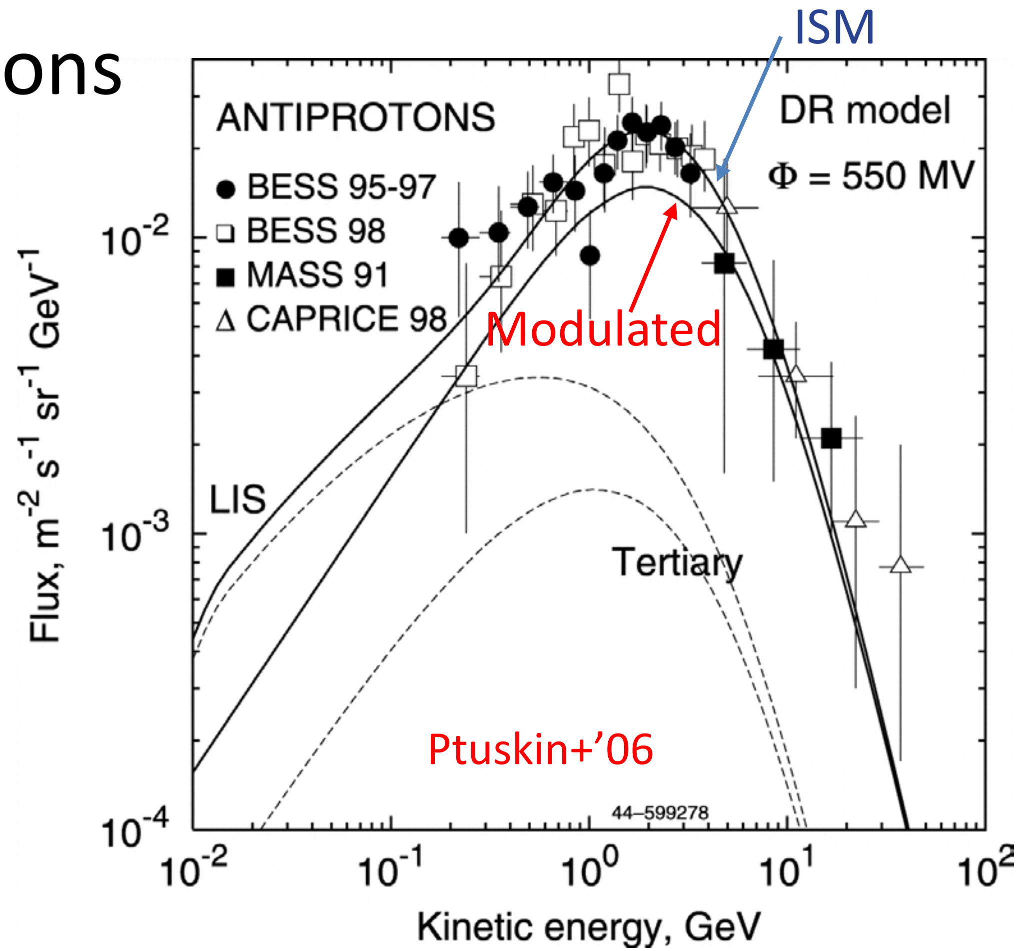

- IM+'02: Secondary Antiprotons and Propagation of Cosmic Rays in the Galaxy and Heliosphere
- IM+'03: Challenging Cosmic-Ray Propagation with Antiprotons: Evidence for a ``Fresh'' Nuclei Component?
- Ptuskin+'06: Dissipation of Magnetohydrodynamic Waves on Energetic Particles: Impact on Interstellar Turbulence and Cosmic-Ray Transport
- Kachelriess+'15: New Calculation of Antiproton Production by Cosmic Ray Protons and Nuclei
- …

AMS-02: solving the GeV $\bar{p}$ excess

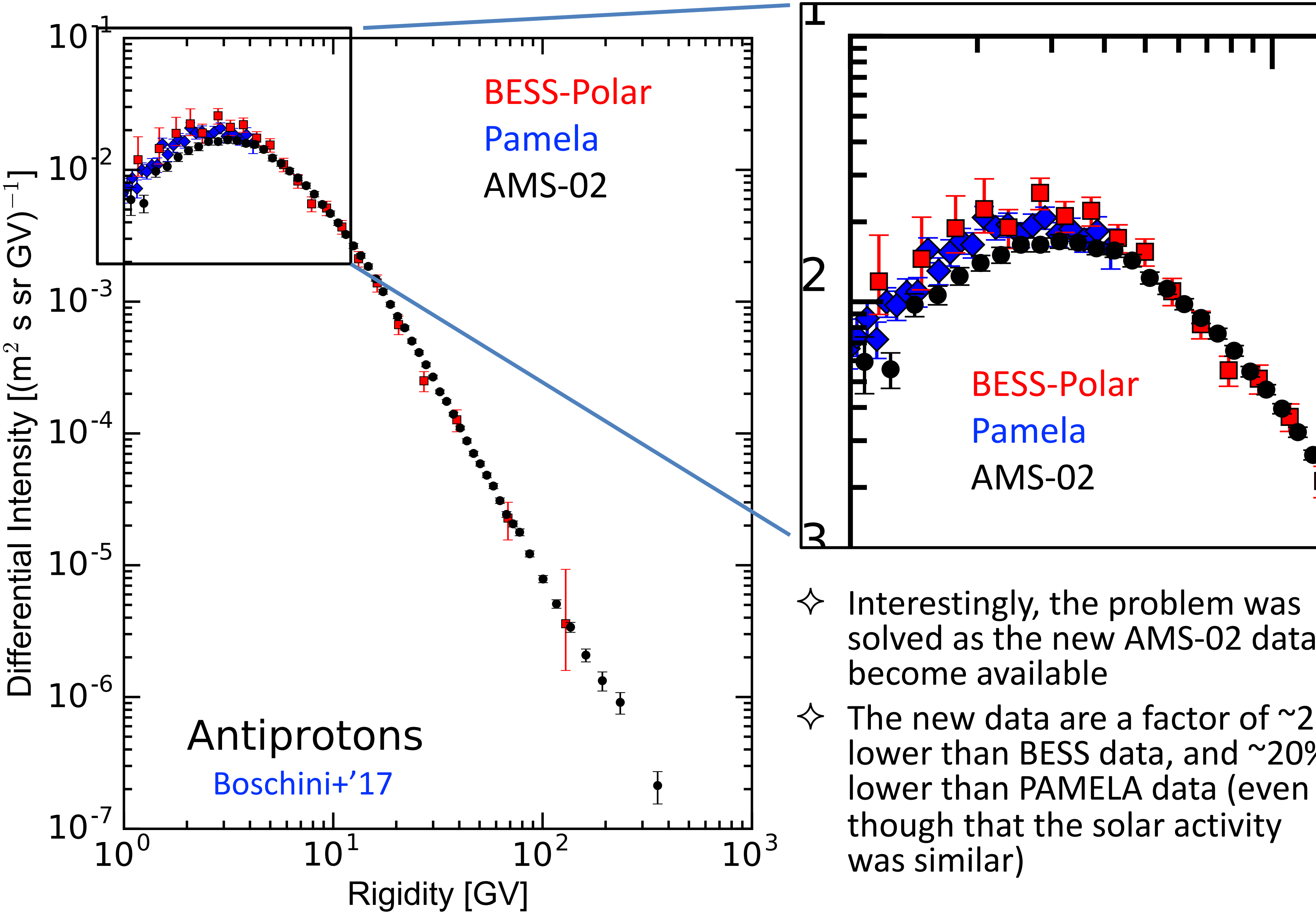

- ✧ Interestingly, the problem was solved as the new AMS-02 data become available
- ✧ The new data are a factor of ~2 lower than BESS data, and ~20% lower than PAMELA data (even though that the solar activity was similar)

AMS-02: 10 GeV $\bar{p}$ excess?

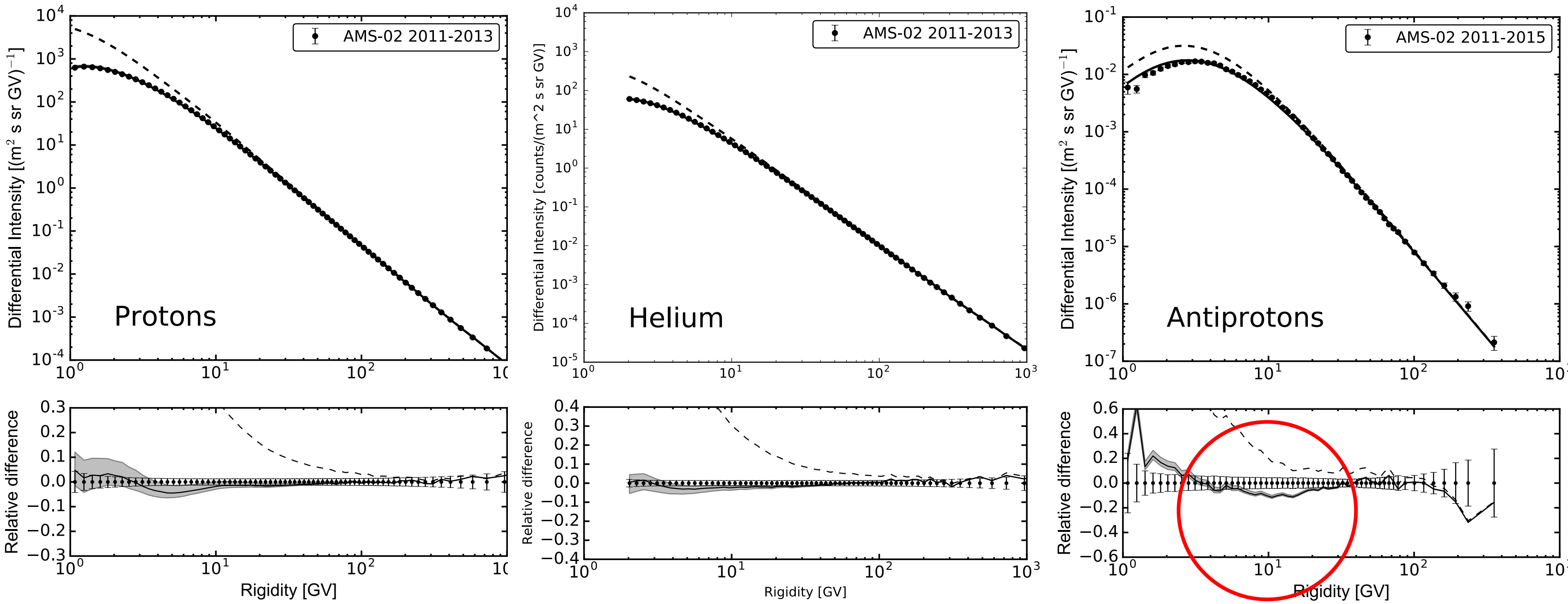

- ✧ CR proton and He data (BESS, PAMELA, AMS-02) are described very well for variety of conditions: low/high/intermediate solar activity
- ✧ The residuals are at ~5% level
- ✧ Antiprotons were not optimized, but agree well with calculations
- ✧ There is a clear excess around ~10 GeV at the level of ~15%
- ✧ True excess or calculation/instrumental systematics?

Fluxes of CR species

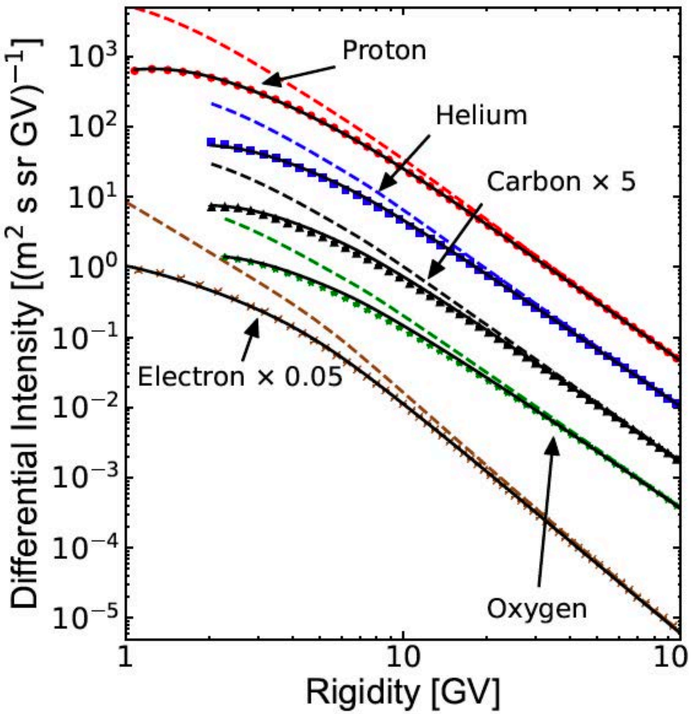

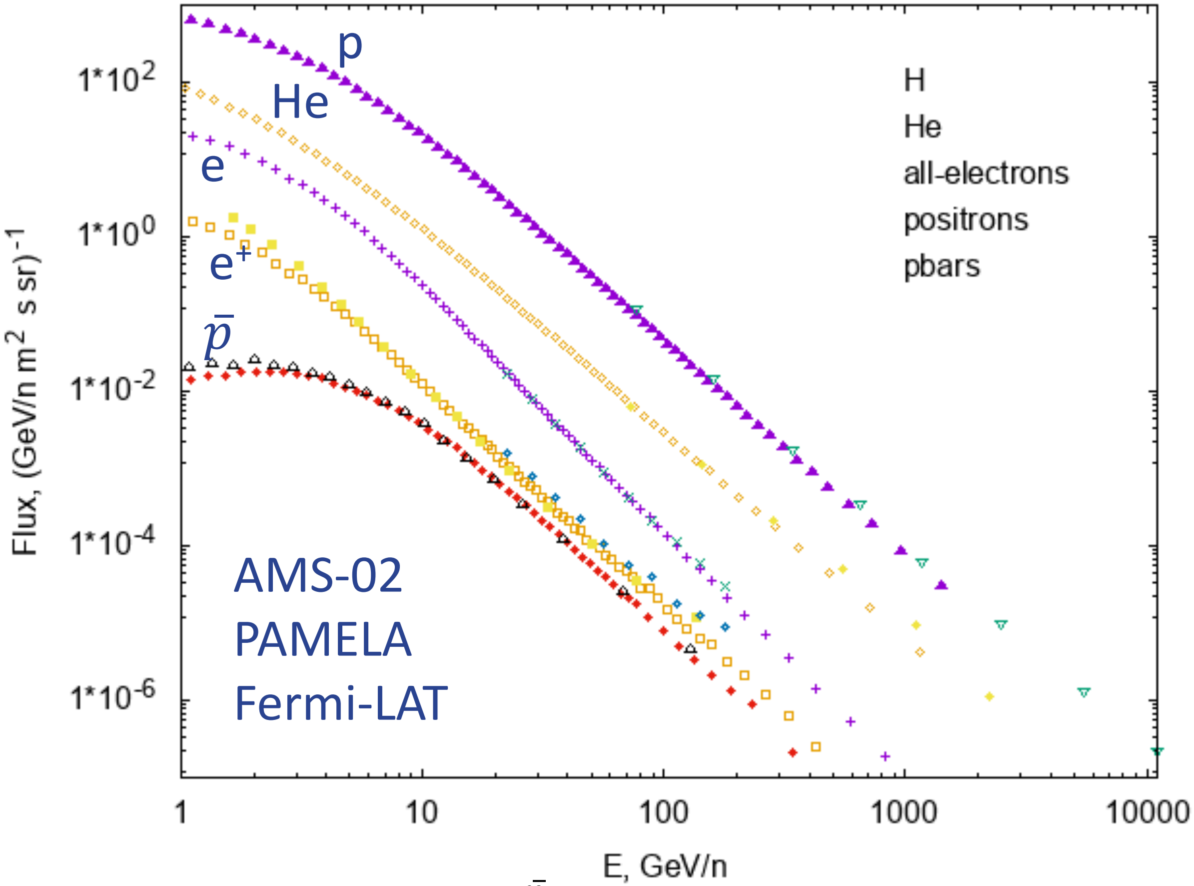

- ✧ The range of intensities is quite spectacular with $\frac{\bar{p}}{p} \sim 10^{-5} \div 10^{-4}$
- ✧ The fluxes drop by 10^{-7} between 1 GeV and 1 TeV!
- ✧ Yet the solar modulation suppresses the fluxes of CR species by an order of magnitude at low rigidities
- ✧ Thanks to CR Data Base by D. Maurin+

Fluxes of CR species

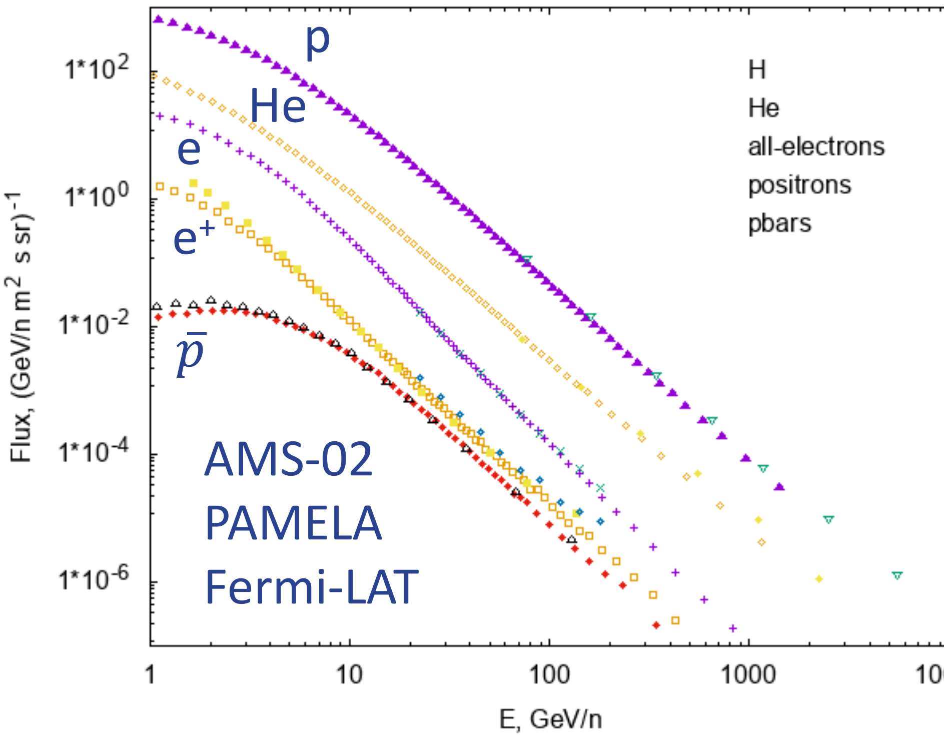

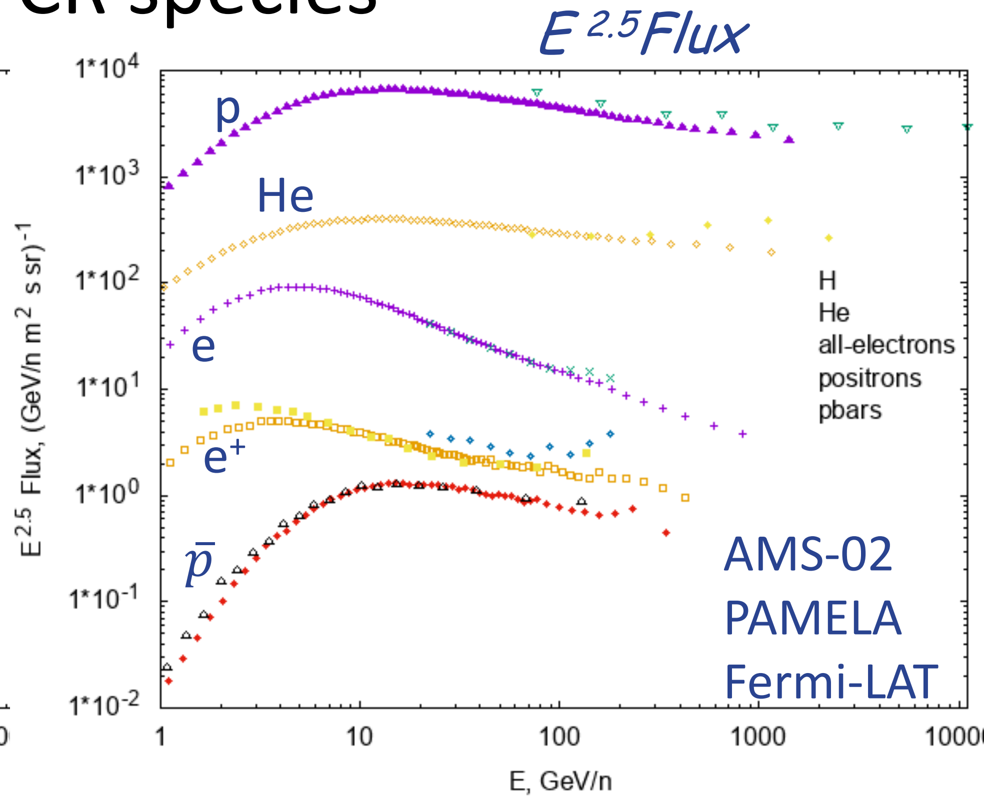

- Changing the scale from *Flux* to *E* $^{2.5}$*Flux* makes a big difference too!
- However, both are important:
  - see the real drop of the flux with energy
  - see the systematics

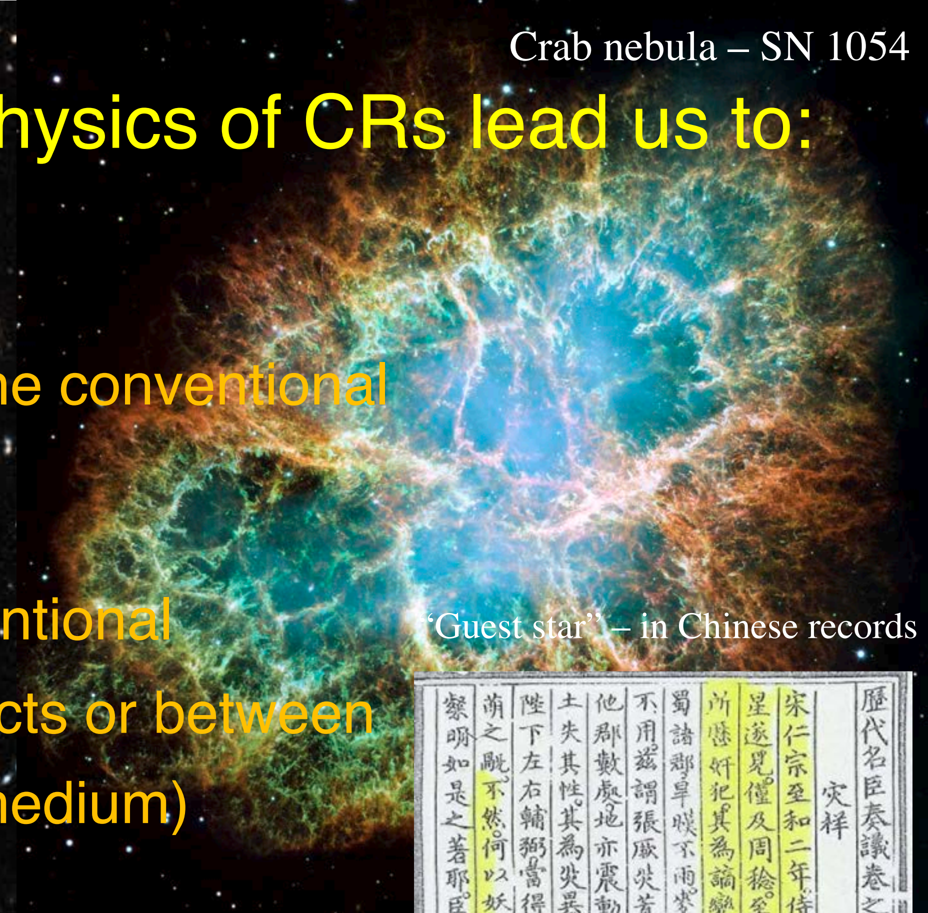

New discoveries in Astrophysics of CRs lead us to:

- ✧ Improve our understanding of the conventional astrophysical backgrounds
- ✧ Provide new insights into conventional processes in astrophysical objects or between them (interstellar/intergalactic medium)
- ✧ Potentially uncover signatures of new/exotic physics that we still have to understand
- ✧ Or to better understanding of the instruments

"Guest star" – in Chinese records

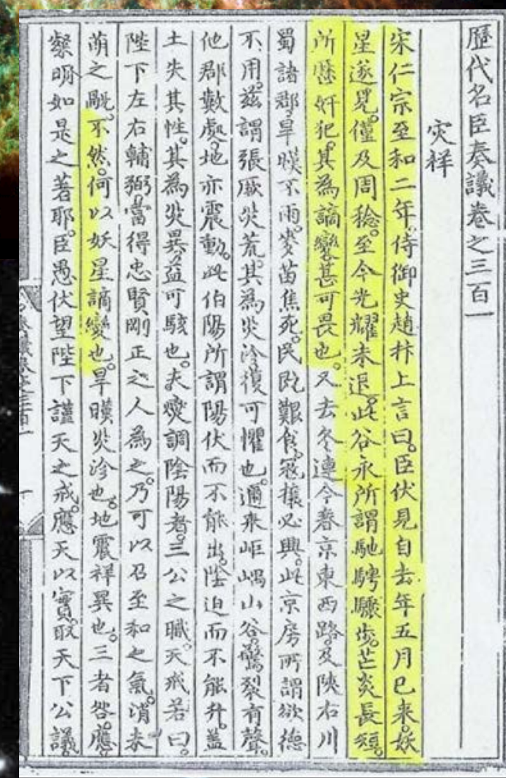
歷代名臣奏議卷之三百一

災祥

宋仁宗至和二年侍御史趙抃上言曰臣伏見自去年五月已來妖
星遂見僅及周歲至今光耀未退此谷永所謂馳騁驟步芒炎長短
所歷奸犯其為譴變甚可畏也又去冬連今春京東西路及陜右川
蜀諸郡旱暵不雨麥苗焦死民既艱食寇攘必興此京房所謂欲德
不用茲謂張厥災荒其為災沴復可懼也邇來岠嵎山谷鷙裂有聲
他郡數處地亦震動此伯陽所謂陽伏而不能出陰迫而不能升蓋
土失其性其為災異益可駭也夫燮調陰陽者三公之職天戒若曰
陛下左右輔弼當得忠賢剛正之人為之乃可以召至和之氣消未
萌之禍不然何以妖星譴變也旱暵災沴也地震祥異也三者咎應
粲明如是之著耶臣愚伏望陛下謹天之戒應天以實取天下公議

Secondary/Primary vs rigidity

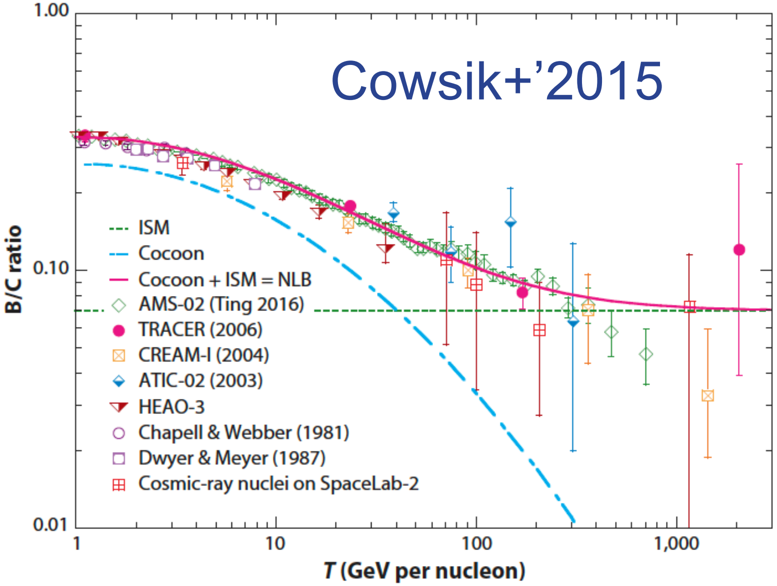

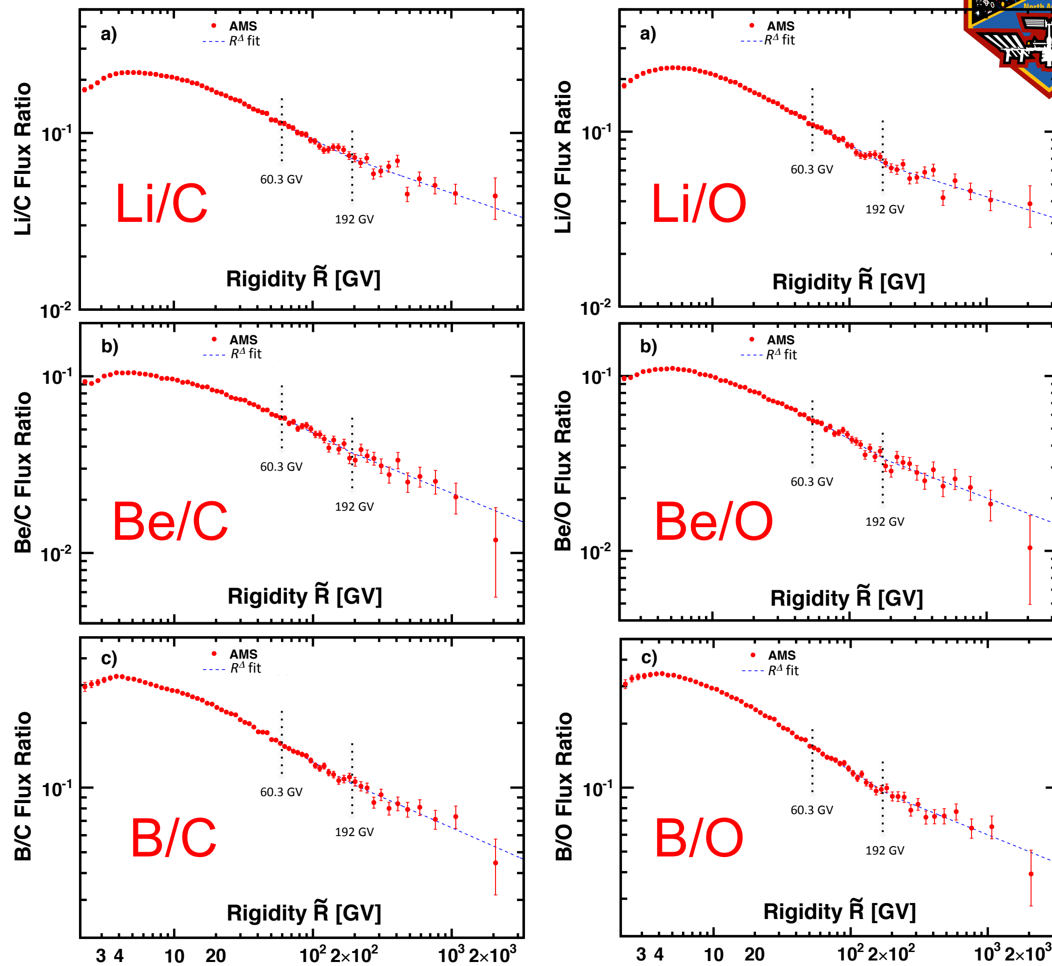

[60.3 GV–192 GV] and
[192 GV–3300 GV]

No flattening or a raise in the secondary/primary is observed
Inconsistent with predictions of the Nested Leaky-Box model

Breaks in the spectra of CR species

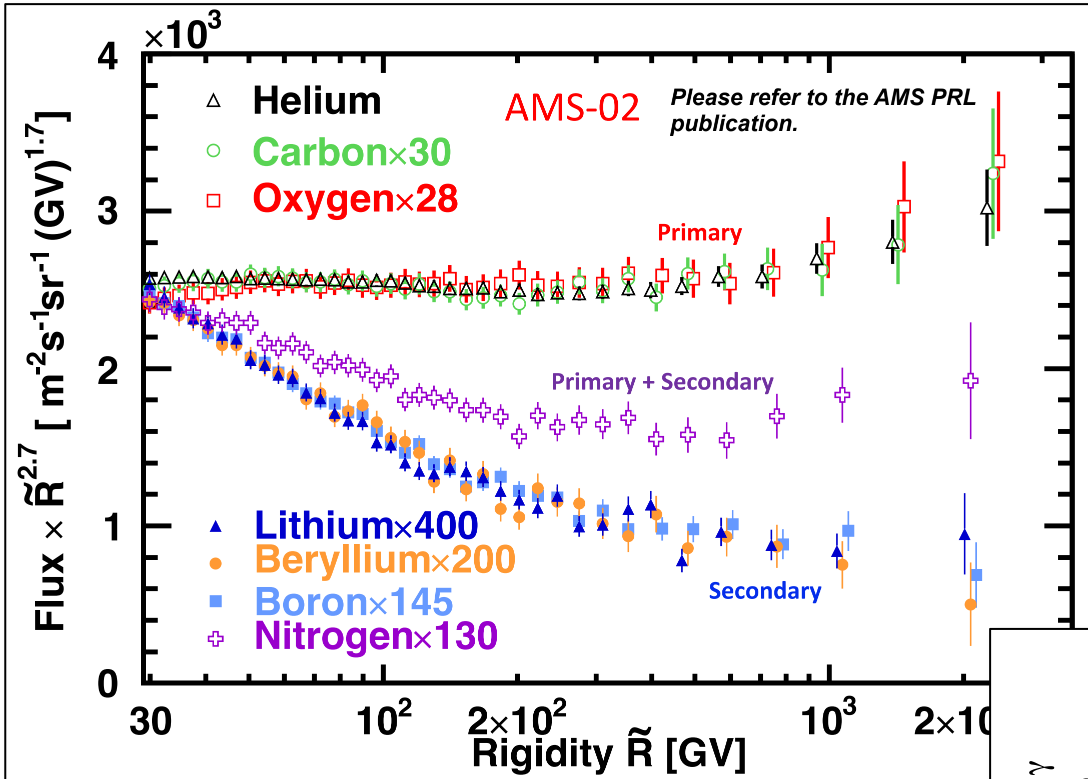

- ◇ Spectra of secondaries are steeper than primaries in the whole energy range – contradictory to the hypothesis of secondary production in SNR shocks
- ◇ Also difficult is to have so well correlated behavior (vs rigidity) of all primary and all secondary species because of very much different fragmentation and production cross sections

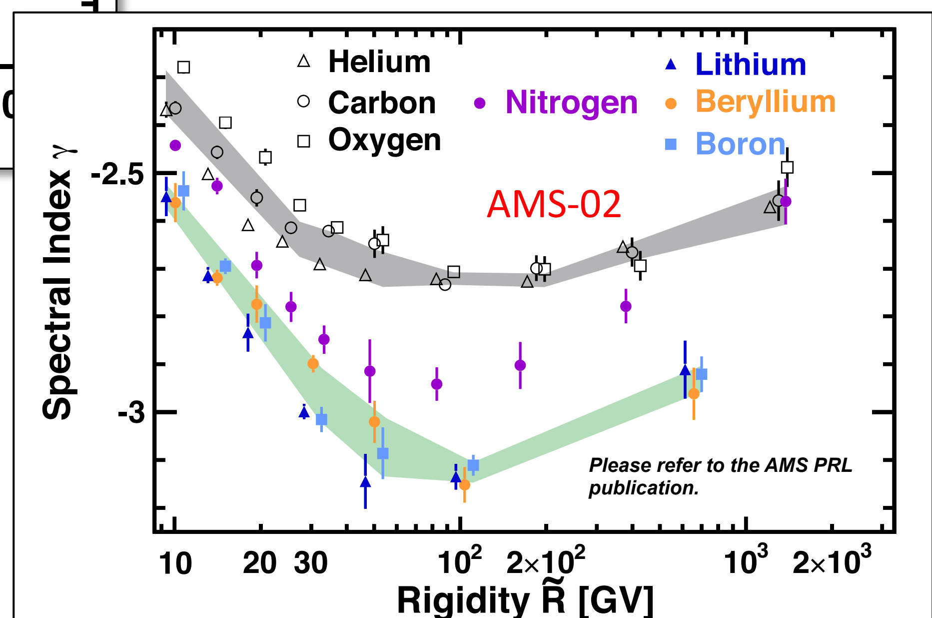

- ◇ More likely and consistent with change in the propagation properties of the interstellar medium, in the diffusion coefficient (Vladimirov+’12)
- ◇ Change in the spectrum of interstellar turbulence (Blasi+’12)

HAWC observations of the extended emission from Geminga & PSR B0656

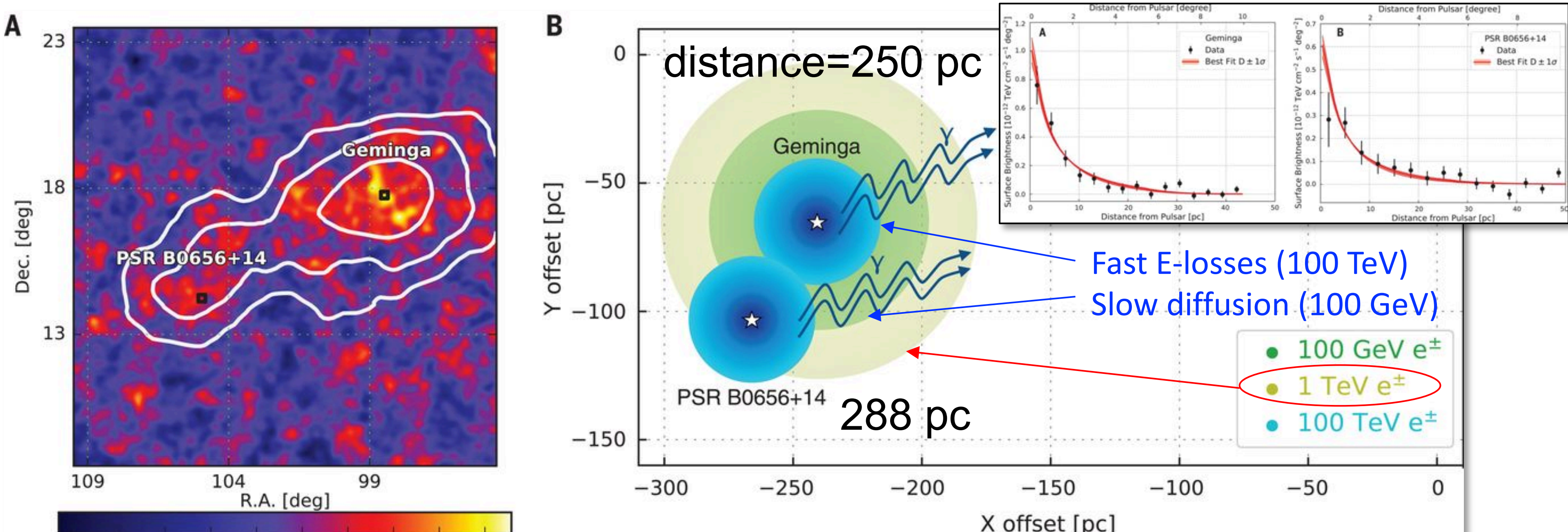

Abeysekara+’2017

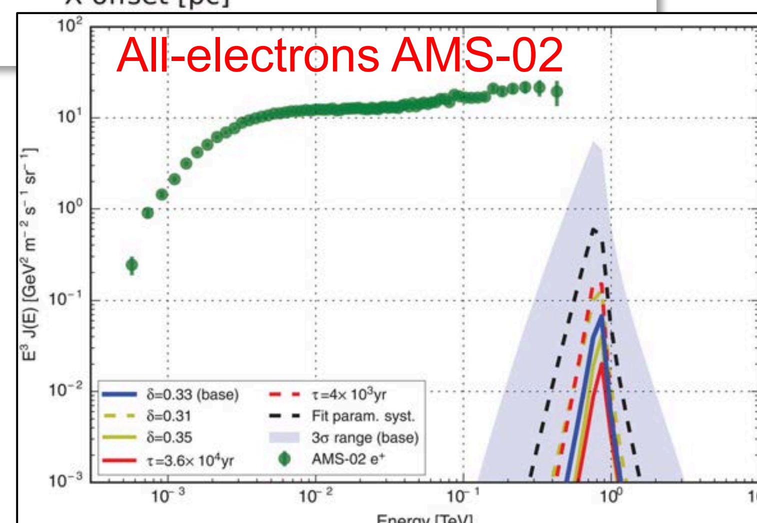

- ✧ Evidence of a non-uniform diffusion near the sources of CRs
- ✧ Fast E-losses (100 TeV) vs slow diffusion (100 GeV)
- ✧ The local value ~4.5×10^{27} cm^2 s^{-1} @100 TeV is << the average from the B/C ratio
- ✧ Proper motion ~60 pc since SN (Geminga)

Spatially Resolved CR diffusion in LMC: 30 Doradus

24 µm (Color) – starforming
1-3 GeV (Contours) – 10-20 GeV p

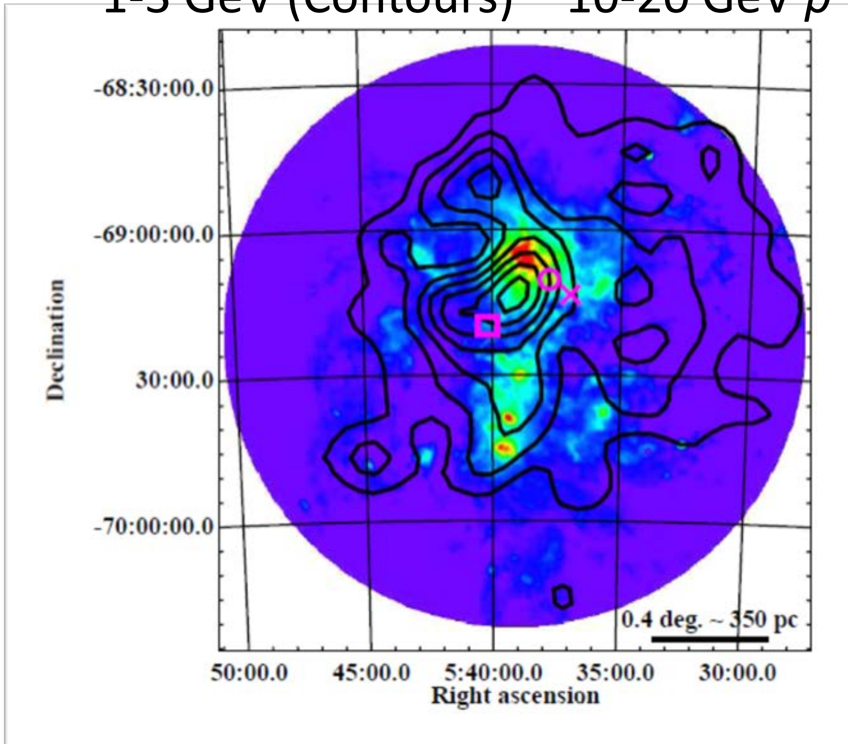

1.4 GHz (Color) – 3 GeV e^-
1-3 GeV (Contours) – 10-20 GeV p

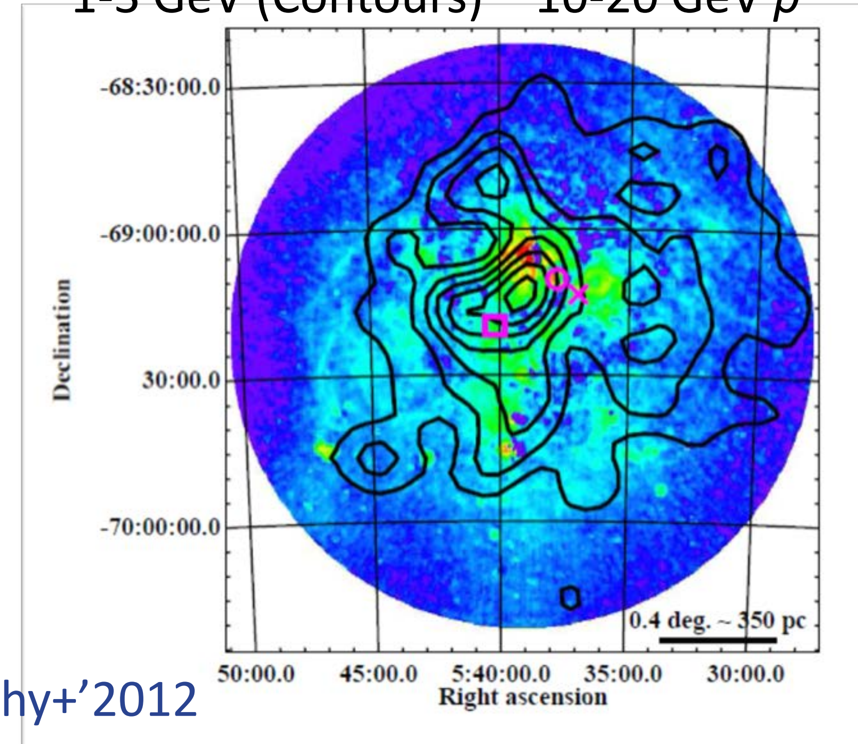

Murphy+'2012

- ✧ IR – proxy for the star forming region (SNR)
- ✧ Radio – synchrotron emission from electrons (100-140 pc at ~3 GeV)
- ✧ Gamma rays – emission from π^0-decay (CR protons, 200-320 pc at ~20 GeV)
- ✧ Diffusion coefficient ~$10^{27}(R/GV)^{0.7}$ cm^2 s^{-1} (~20 times lower than average in the MW)

Excitation of turbulence by the leaking particles

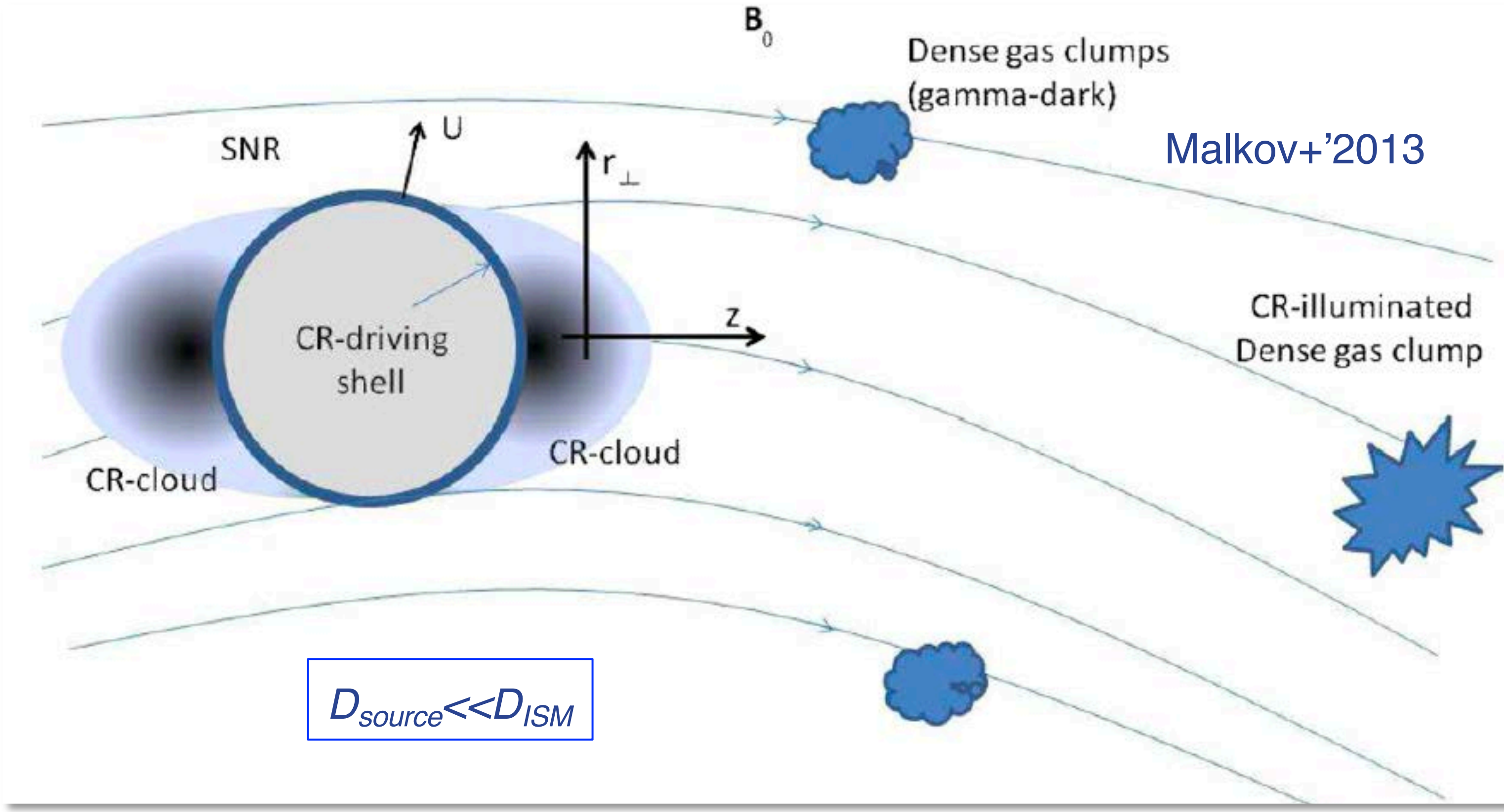

- ✧ Escaping CRs excite the Alfvén waves (Ptuskin+'08; Malkov+'13; D'Angelo+'16)
- ✧ The diffusion coefficient is strongly suppressed compared to its background ISM value

Starforming Galaxies (Fermi-LAT)

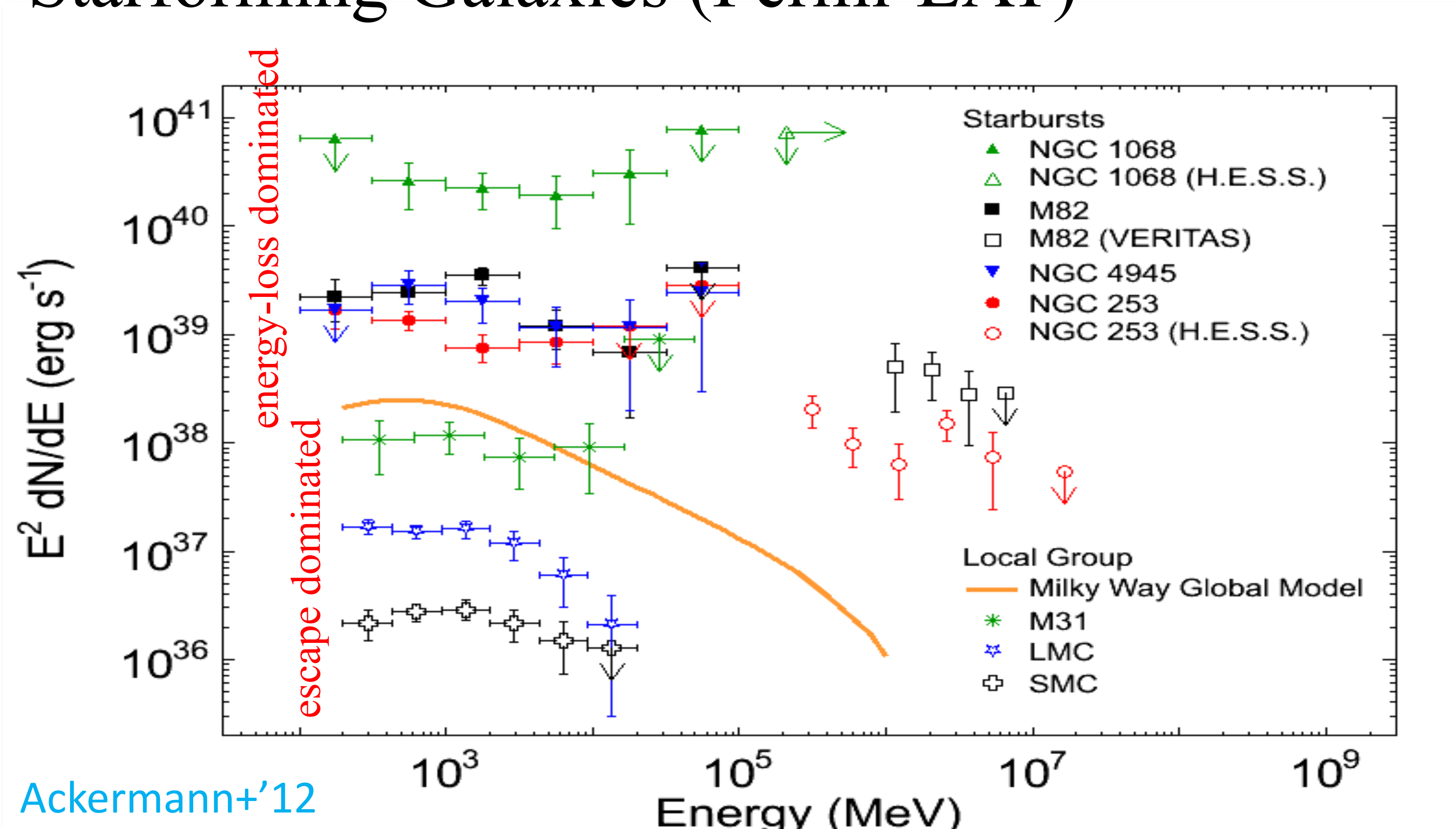

- ✧ Spectral flattening becomes obvious when the energy losses of CR particles (starburst galaxies) start dominating the losses due to the escape (MW, M31, LMC, SMC)
- ✧ Interstellar medium becomes very turbulent, small diffusion coefficient

Cosmic Rays as a Universal Phenomenon

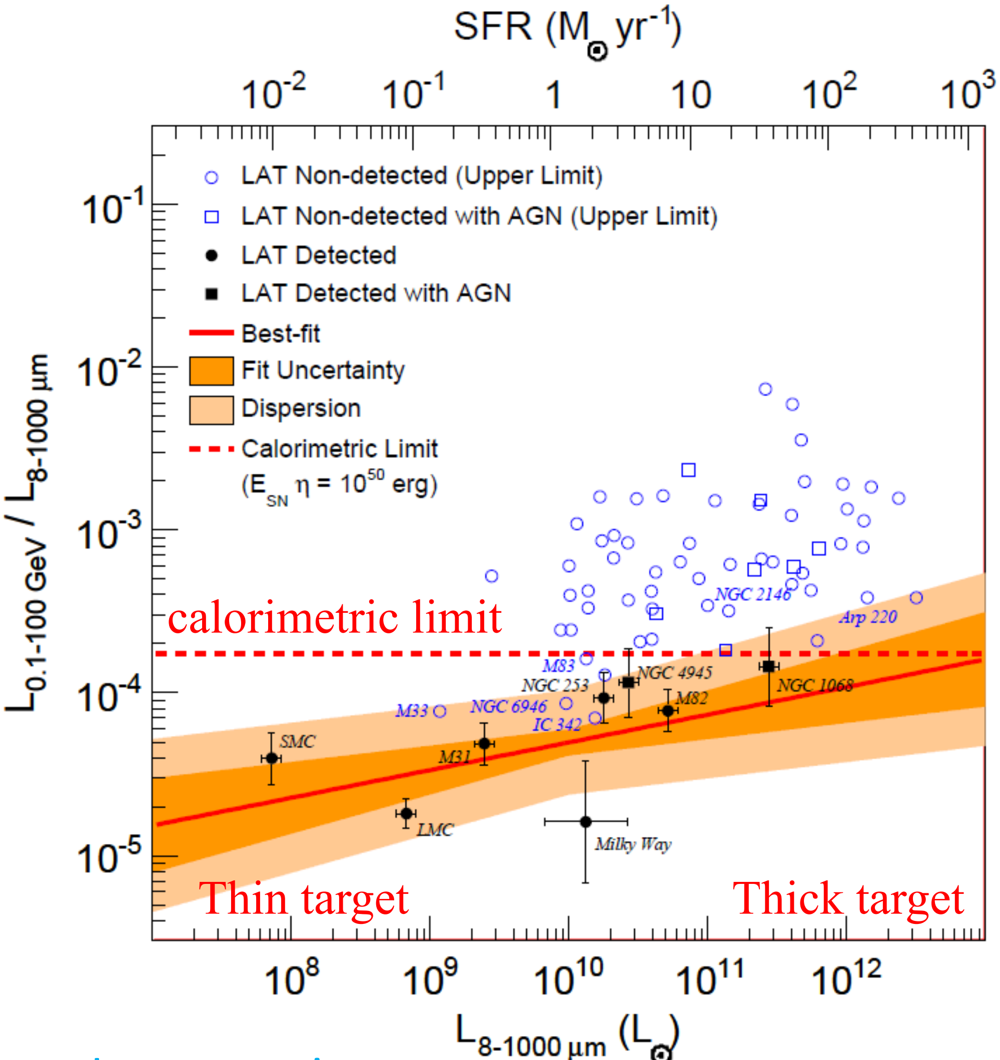

Ackermann+'12

- ✧ γ-ray luminosity vs. IR luminosity for normal galaxies detected with Fermi-LAT
- ✧ The γ-ray luminosity scales linearly (index ~1.1) with the total emission of hot stars reprocessed by dust – a tracer of star formation
- ✧ The ratio approaches the calorimetric limit in star-burst galaxies
- ✧ An evidence of the SNR-CR connection in normal star-forming galaxies

e^+ and γ from Geminga (2-zone model)

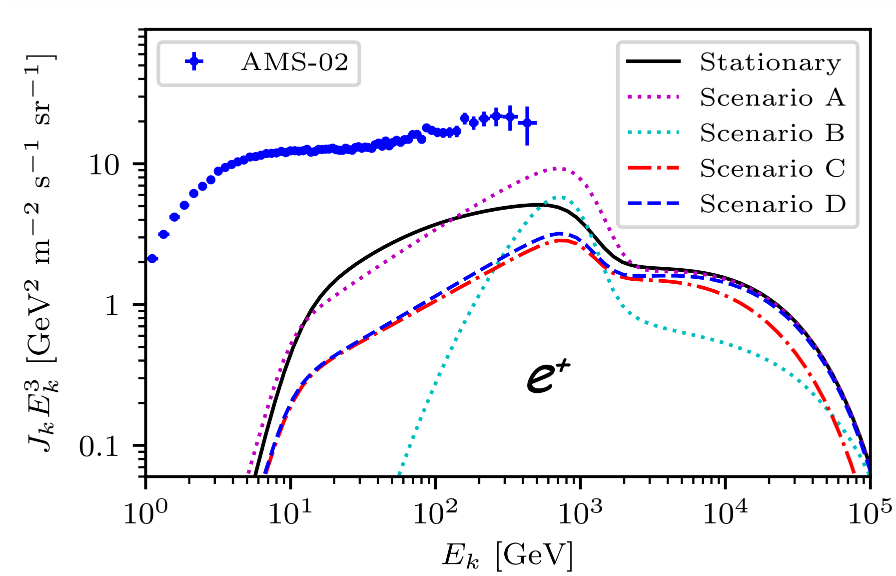

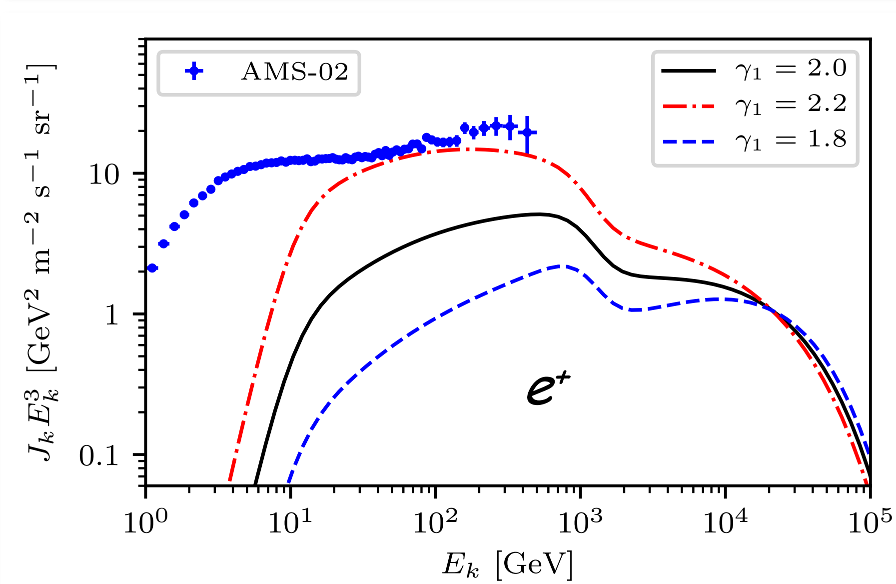

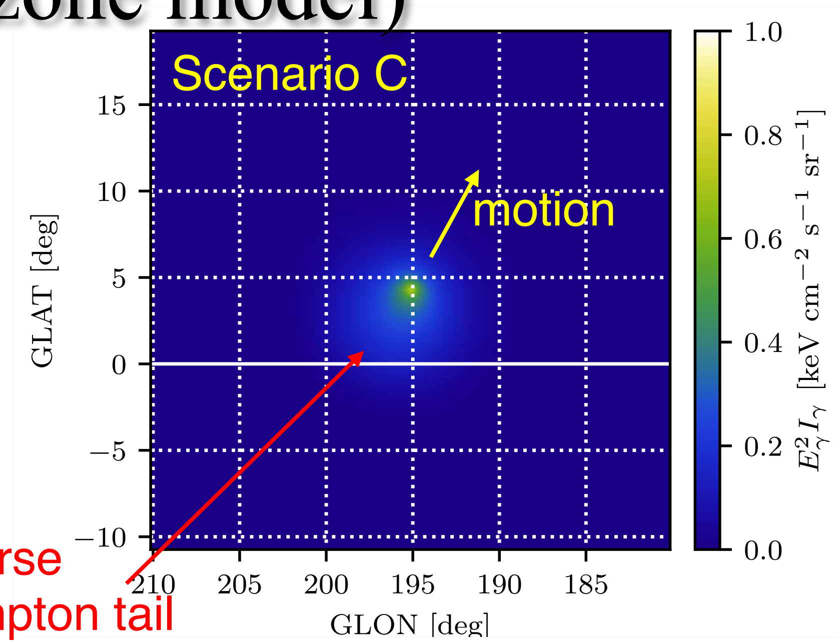

Inverse Compton tail (10 GeV)

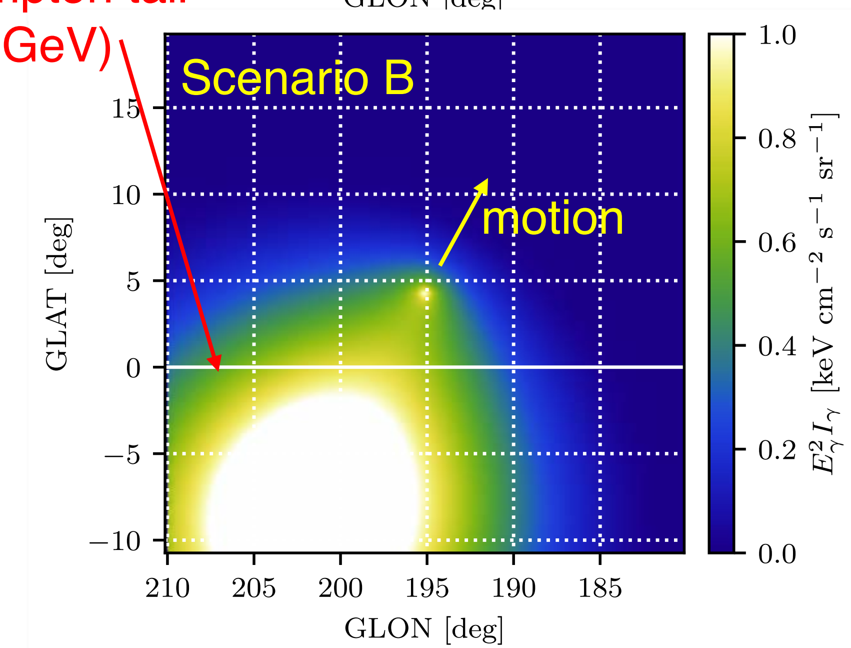

(also Profumo+,Tang&Piran, Fang+, Evoli+'18)

Johannesson+'19, arXiv: 1903.05509

Generalization to the whole MW galaxy

Distribution of the effective diffusion coefficient in 2D and 3D model

Johannesson+'19, arXiv: 1903.05509

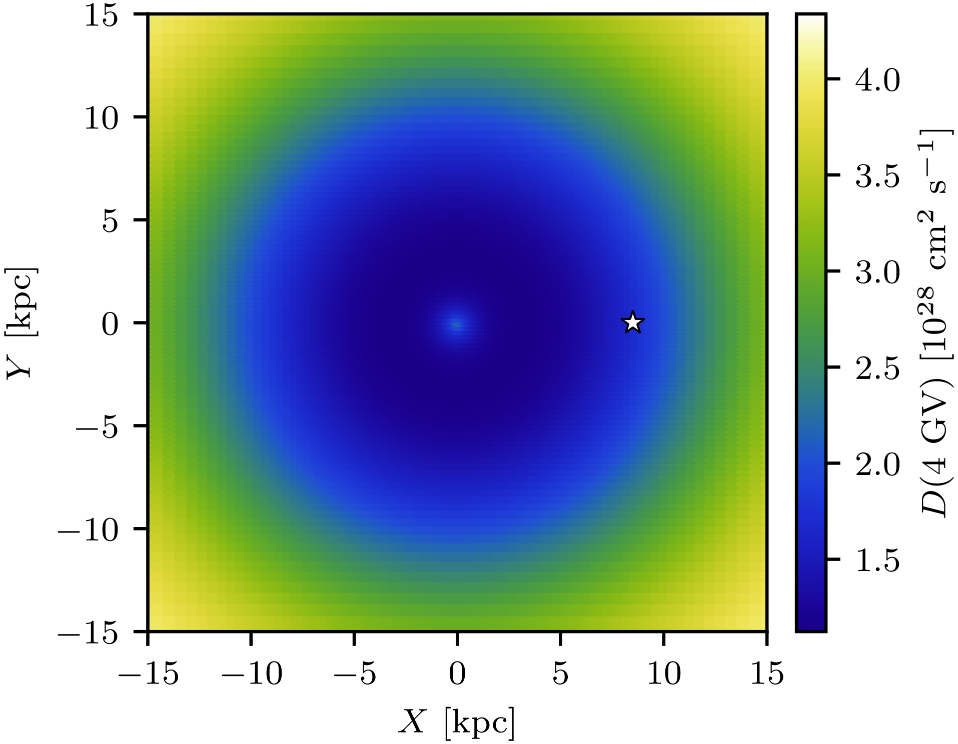

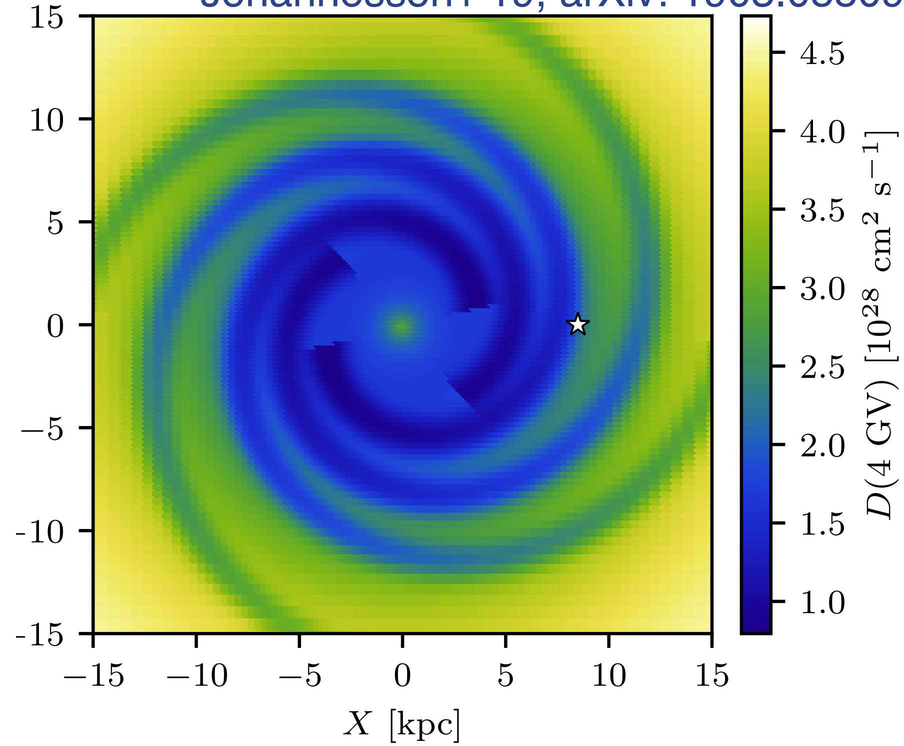

- Assuming the slow diffusion zone around each CR source, the effective diffusion coefficient in the plane may vary by a factor of 2-3
- Produces relatively small effect on CR spectra – diffusion coefficient in the halo remains unaltered
- Effect on the diffuse emission is still being evaluated

Diffusion coefficient may vary…

We've just learned:

- ✧ Its rigidity dependence may be different at low and high energies
- ✧ Its spatial dependence may be quite complicated (sources, B-field, etc.)
- ✧ But e^- and e^+ behave quite differently from other CR species!

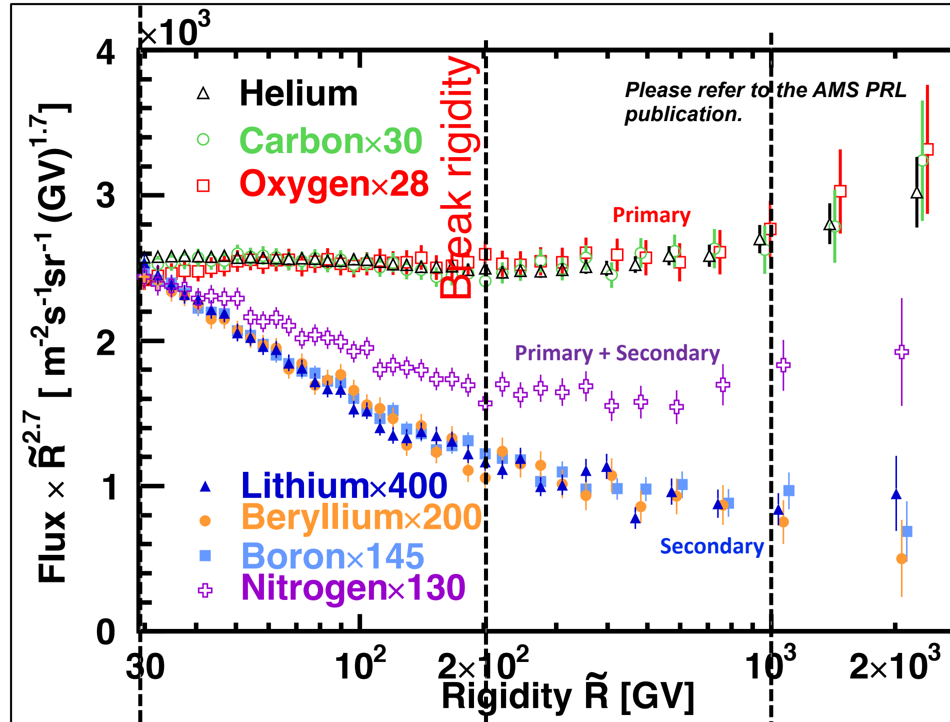

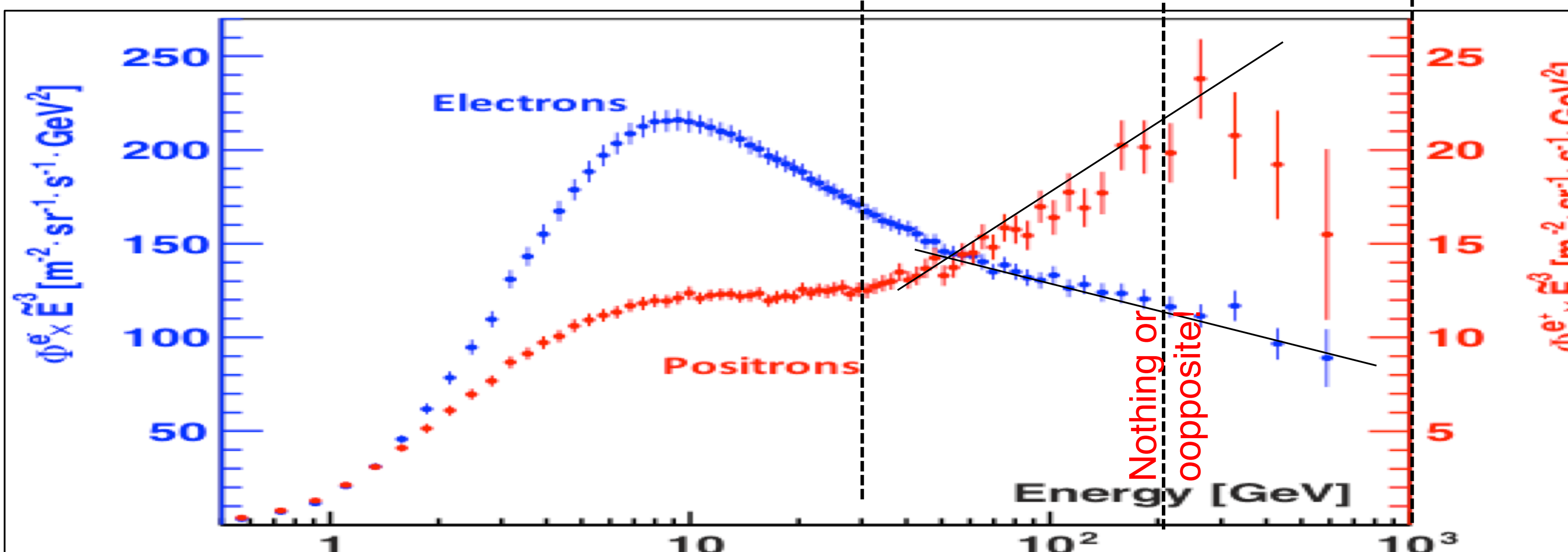

Crab nebula – SN 1054

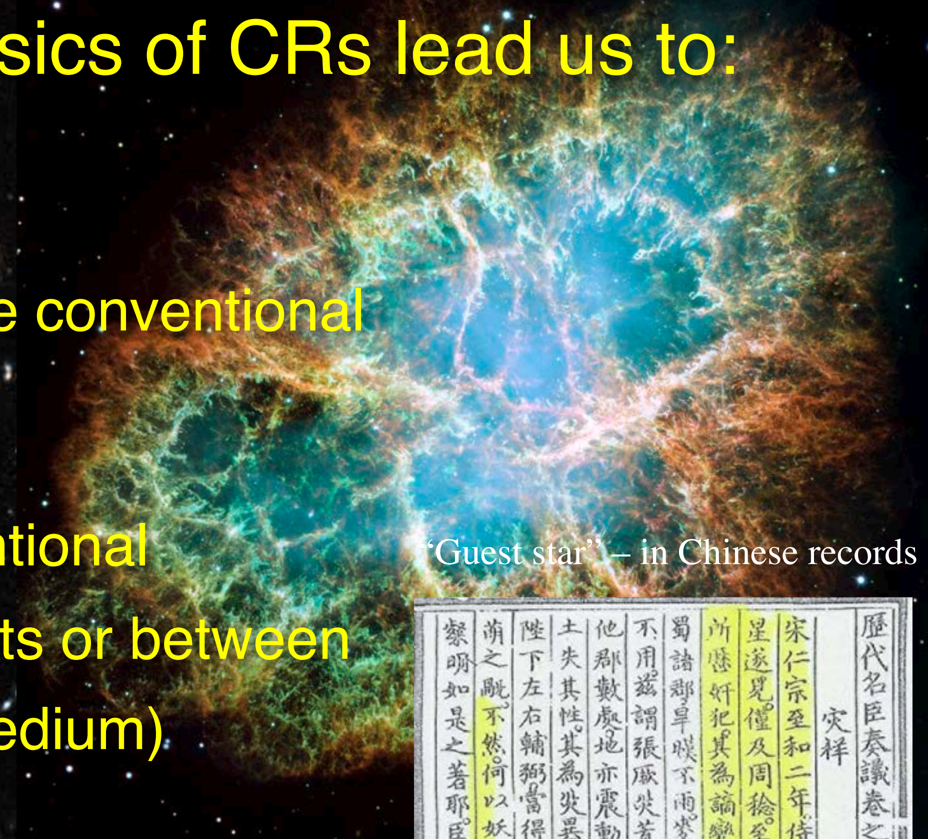

New discoveries in Astrophysics of CRs lead us to:

- ✧ Improve our understanding of the conventional astrophysical backgrounds
- ✧ Provide new insights into conventional processes in astrophysical objects or between them (interstellar/intergalactic medium)
- ✧ Potentially uncover signatures of new/exotic physics that we still have to understand
- ✧ Or to better understanding of the instruments

"Guest star" – in Chinese records

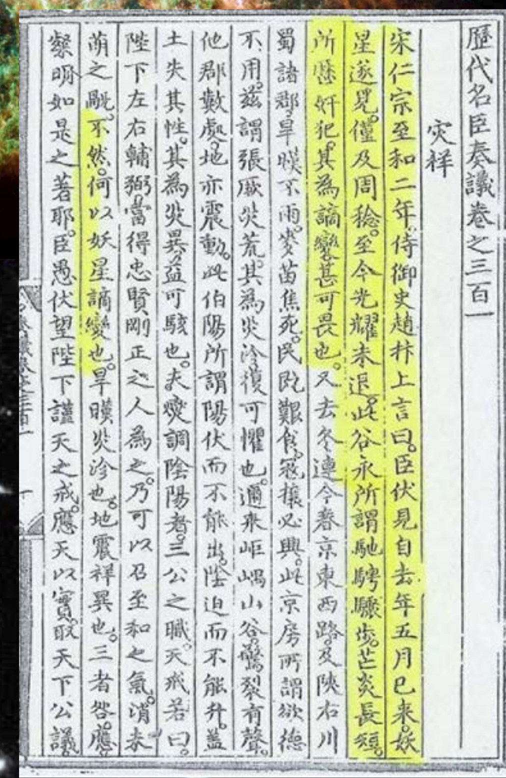

歷代名臣奏議卷之三百一

災祥

宋仁宗至和二年侍御史趙抃上言曰。臣伏見自去年五月巳來妖星遂見。僅及周稔。至今光耀未退。此谷永所謂馳騁驟步芒炎長短。所懸奸犯其為譎變甚可畏也。又去冬連今春京東西路及陝右川蜀諸郡旱暵不雨。麥苗焦死。民既艱食。寇攘必興。此京房所謂欲德不用。茲謂張厥災荒。其為災沴復可懼也。邇來岷峨山谷。驚裂有聲。他郡數處地亦震動。此伯陽所謂陽伏而不能出。陰迫而不能升。蓋土失其性。其為災異益可駭也。夫變調陰陽者。三公之職。天戒若曰。陛下左右輔弼當得忠賢剛正之人為之。乃可以召至和之氣。消殄萌之亂。不然。何以妖星譎變也。旱暵災沴也。地震祥異也。三者咎應粲明如是之著耶。臣愚伏望陛下謹天之戒。應天以實。取天下公議

Fermi Gamma-ray Space Telescope

M31 and its halo (what and why)

See Karwin+, today's arXiv:1903.10533

A brief observational history

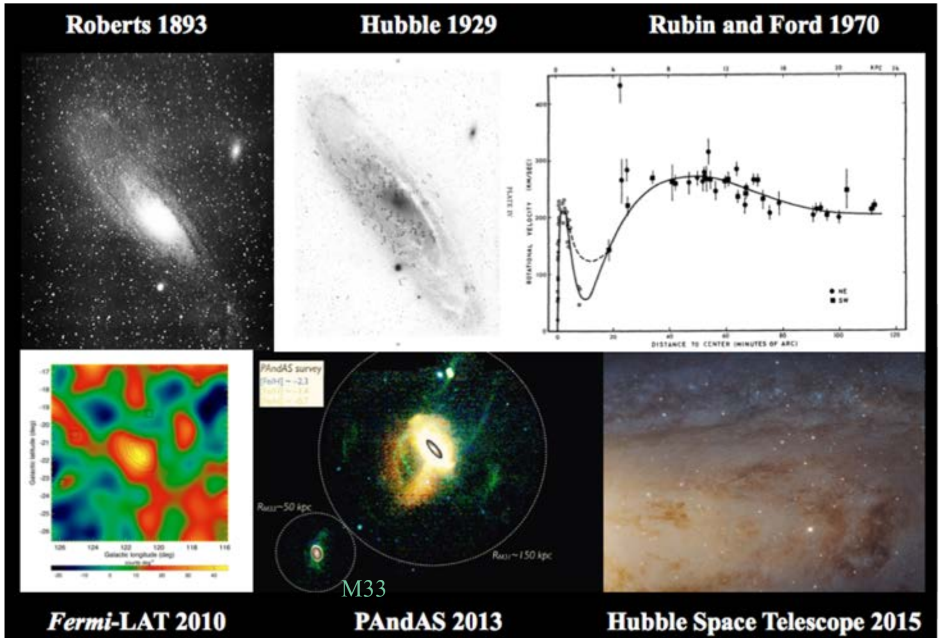

Our region of interest is similar to PAndAS

The big picture (illustrative)

MW-M31-Like Pairs (for example) from Garrison-Kimmel et al. 2018 (link)

- ◇ The closest spiral galaxy and has been the subject of numerous studies
- ◇ Harbors a massive DM halo, may span up to ~600 kpc across and comprises ~90% of the total mass
- ◇ Halo size translates into the diameter of 42° on the sky for M31-Milky Way (MW) distance of 785 kpc, but its presumably low surface brightness makes it challenging to detect with gamma-ray telescopes
- ◇ The entire M31 DM halo is seen from the outside, so we see the extended integral signal. For the MW we see through the halo, so it can be easily confused with diffuse components.

Observations

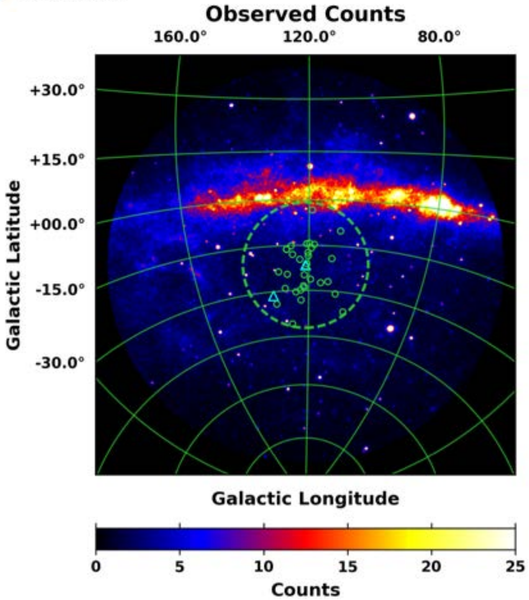

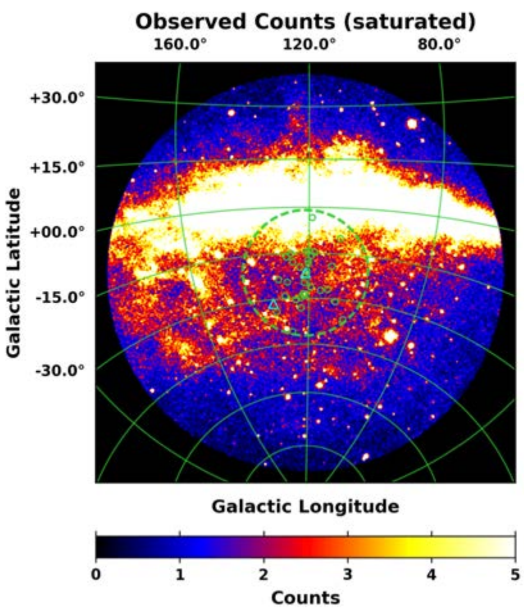

Event Selection:

- Front and back events, P8R2_Clean_V6 selection
- Data: 7.6 years (2008-08-04 to 2016-03-16)
- Full ROI is a 60° radius centered at the position of M31 (l,b) = (121.17°,-21.57°). Our primary field of interest, FM31, is a 28° x 28° region centered at M31.
- Energy range: 1-100 GeV in 20 bins logarithmically spaced
- Pixelation: 0.2° x 0.2°
- Fermi-LAT Science Tools v10-00-05 (run on UCI HPC, v10r0p5)

Images:

- Top: full count range. Bottom: saturated counts, emphasizing lower counts at high latitudes.
- Dashed green circle (21° in radius) corresponds to a 300 kpc projected radius, for an M31-MW distance of 785 kpc, i.e. the virial radius.
- M31 and M33 are shown with cyan triangles, and the rest of M31's dwarf galaxy population are shown with small green circles.
- **The primary purpose of the overlay is to provide a qualitative representation of M31's outer halo and to show its relationship to the MW disk.**
- Note: we do not expect to detect most of the M31 dwarfs, as the MW dwarfs are mostly undetected.

GALPROP Parameters/foreground emission

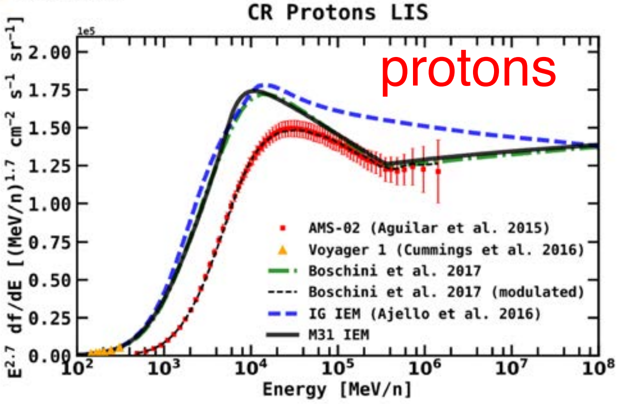

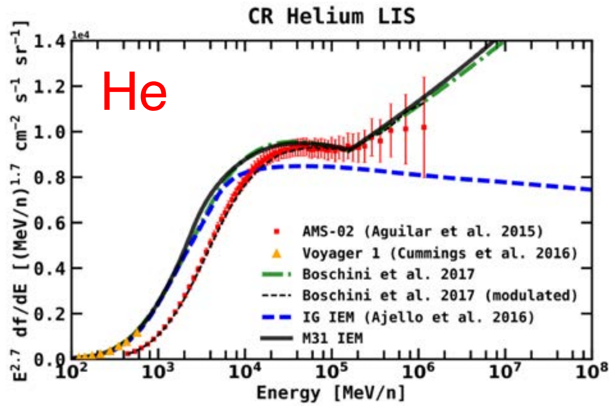

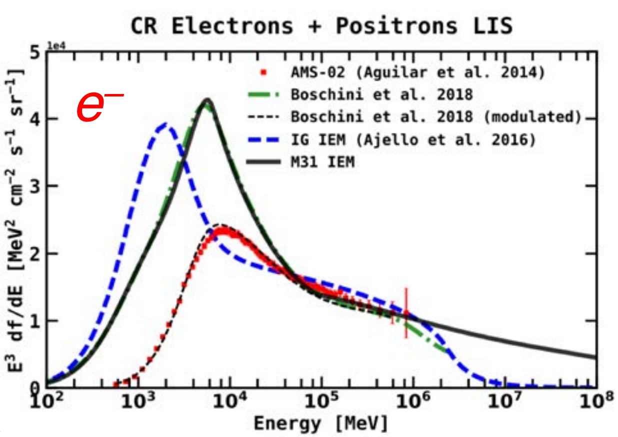

Table 1
GALPROP Model Parameters

Parameter	M31 IEM	IG IEM
[a] z [kpc]	4	6
[a] r [kpc]	20	30
[b] a	1.5	1.64
[b] b	3.5	4.01
[b] r_1	0.0	0.55
[c] D_0 [10^{28} cm^2 s^{-1}]	4.3	7.87
[c] δ	0.395	0.33
[c] η	0.91	1.0
[c] Alfvén speed, v_A [km s^{-1}]	28.6	34.8
[d] $v_{\rm conv,0}$ [km s^{-1}]	12.4	...
[d] $dv_{\rm conv}/dz$ [km s^{-1} kpc^{-1}]	10.2	...
[e] $R_{p,0}$ [GV]	7	11.6
[e] $R_{p,1}$ [GV]	360	...
[e] $\gamma_{p,0}$	1.69	1.90
[e] $\gamma_{p,1}$	2.44	2.39
[e] $\gamma_{p,2}$	2.295	...
[e] $R_{\rm He,0}$ [GV]	7	...
[e] $R_{\rm He,1}$ [GV]	330	...
[e] $\gamma_{\rm He,0}$	1.71	...
[e] $\gamma_{\rm He,1}$	2.38	...
[e] $\gamma_{\rm He,2}$	2.21	...
[e] $R_{e,0}$ [GV]	0.19	...
[e] $R_{e,1}$ [GV]	6	2.18
[e] $R_{e,2}$ [GV]	95	2171.7
[e] $\gamma_{e,0}$	2.57	...
[e] $\gamma_{e,1}$	1.40	1.6
[e] $\gamma_{e,2}$	2.80	2.43
[e] $\gamma_{e,3}$	2.40	4.0
[f] J_p [10^{-9} cm^{-2} s^{-1} sr^{-1} MeV^{-1}]	4.63	4.0
[f] J_e [10^{-11} cm^{-2} s^{-1} sr^{-1} MeV^{-1}]	1.44	0.011
[g] A5 [kpc]	8–10	8–10
[g] A6 [kpc]	10–11.5	10–50
[g] A7 [kpc]	11.5–16.5	...
[g] A8 [kpc]	16.5–50	...
[h] IC Formalism	Anisotropic	Isotropic

Boschini+'17,18

Note. — For reference, we also give corresponding values for the ("Yusifov") IEMs used in Ajello et al. (2016) for the analysis of the inner Galaxy (IG).

[a] Halo geometry: z is the height above the Galactic plane, and r is the radius.
[b] CR source density. The parameters correspond to Eq. (1).
[c] Diffusion: $D(R) \propto \beta^\eta R^\delta$. $D(R)$ is normalized to D_0 at 4.5 GV.
[d] Convection: $v_{\rm conv}(z) = v_{\rm conv,0} + (dv_{\rm conv}/dz)z$.
[e] Injection spectra: The spectral shape of the injection spectrum is the same for all CR nuclei except for protons. The parameters correspond to Eq. (2).
[f] The proton and electron flux are normalized at the Solar location at a kinetic energy of 100 GeV. Note that for the IG IEM the electron normalization is at a kinetic energy of 25 GeV.
[g] Boundaries for the annuli which define the IEM. Only A5 (local annulus) and beyond contribute to the foreground emission for FM31.
[h] Formalism for the inverse Compton (IC) component.

Source Density (top) and

Injection Spectrum (bottom)

$$\rho(r) = \left(\frac{r + r_1}{r_\odot + r_1}\right)^a \times \exp\left(-b \times \frac{r - r_\odot}{r_\odot + r_1}\right)$$

$$q(R) \propto (R/R_0)^{-\gamma_0} \prod_{i=0}^{2} \left[1 + (R/R_i)^{\frac{\gamma_i - \gamma_{i+1}}{s_i}}\right]^{s_i}$$

- GALPROP-based (v56) combined diffusion-convection-reacceleration model with a uniform spatial diffusion coefficient and a single power law index over the entire rigidity range.
- Injection and diffusion parameters are derived from local CR measurements, including AMS-02 and Voyager 1.
- Use the GALPROP parameters from Boschini et al. 2017,2018, which employ GALPROP and HelMod.
- CR source density based on the distribution of pulsars.
- IG IEM from Ajello et al. 2016 used as a reference model in our study of the systematics for the M31 field.

Interstellar Emission Model

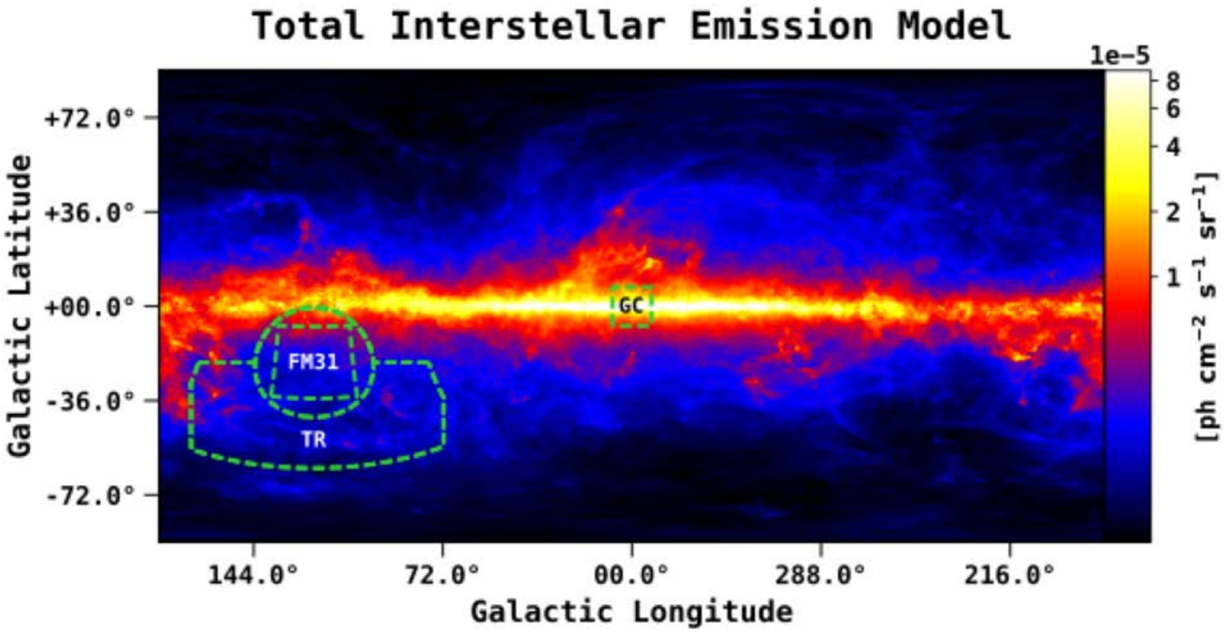

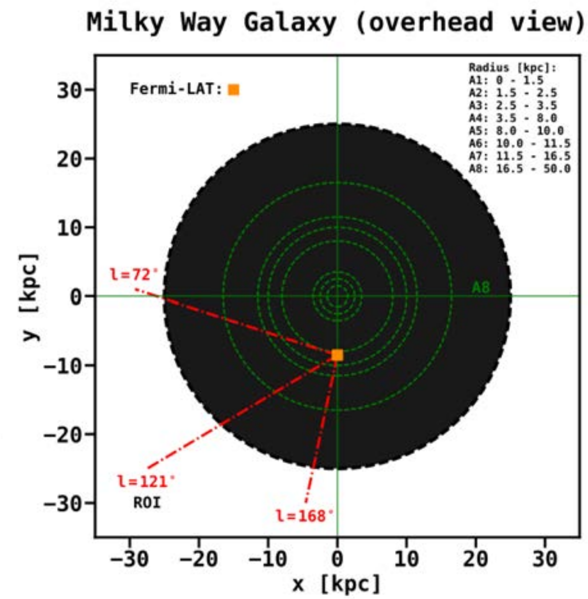

- Total IEM for the MW integrated between 1-100 GeV.
- The color corresponds to the intensity and is shown in log scale. The intensity level corresponds to the initial GALPROP output, before tuning to the gamma-ray data.
- IEM has contributions from pi-0 decay, (anisotropic) IC emission, and Bremsstrahlung emission (see next slide).
- IEM is defined in Galactocentric annuli (A1-A8), but only A5-A8 contribute to the foreground emission towards M31.
- The green dashed circle corresponds to M31's virial radius. Our primary field of interest, FM31, lies within the virial radius, and we use the region outside (and below latitudes of -21.5°) as a tuning region (TR).
- For reference we also show the GC region, which corresponds to a 15° x 15° square centered at the GC.

Interstellar Emission Model

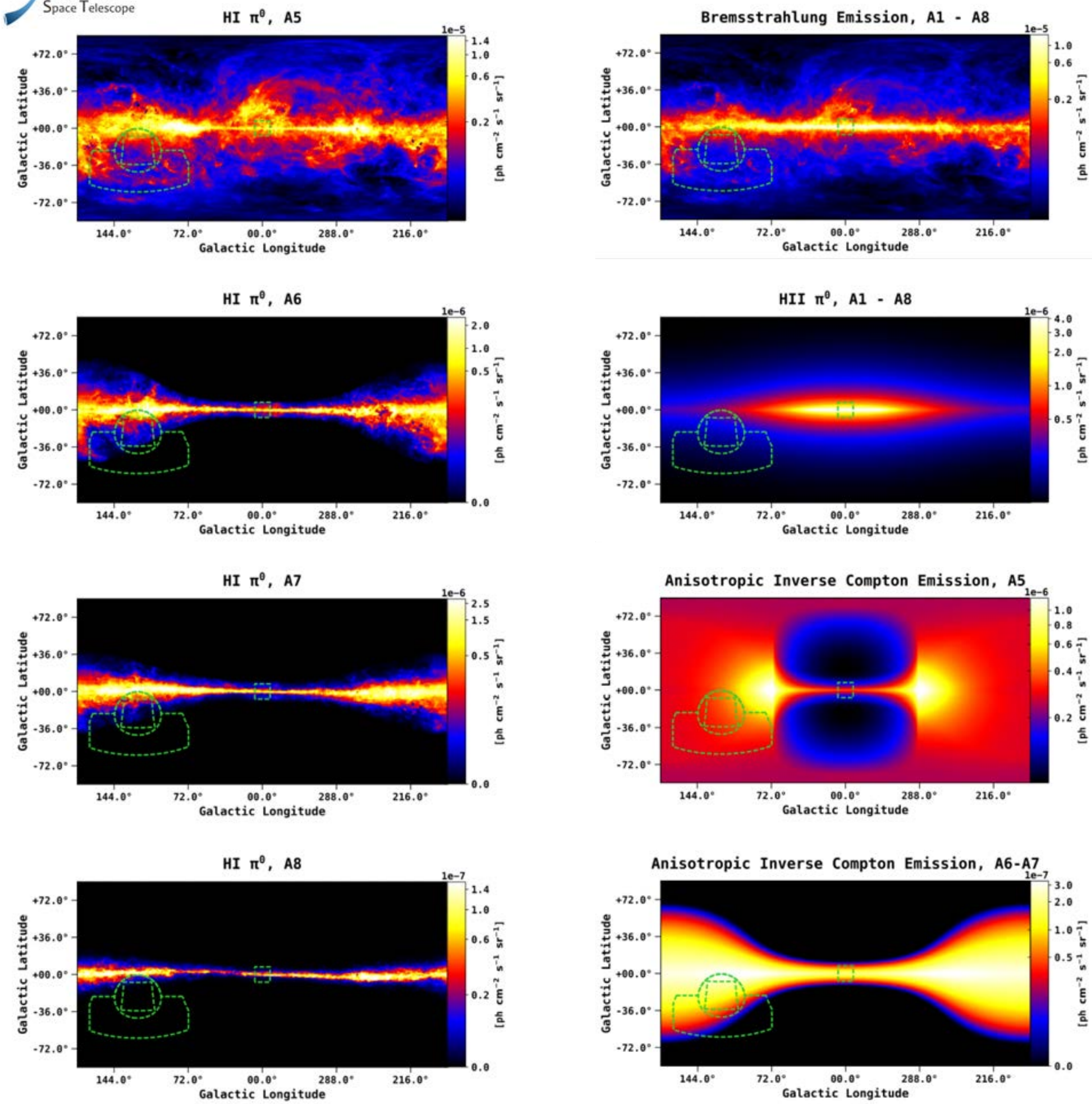

- FM31 has a significant contribution from emission related to H I gas, but there is very little contribution for H2 gas.
- H I map GALPROP employs is based on LAB+GASS data, which for our ROI corresponds to LAB data only.
- A uniform spin temperature of 150 K is assumed.
- Our model also accounts for the dark neutral medium.
- The distribution of He in the interstellar gas is assumed to follow that of hydrogen, with a He/H ratio of 0.11 by number.
- Anisotropic formalism used for IC calculation.
- H I A5 and IC A5 are the dominant contributions in FM31 below ~5 GeV.
- IC A8 has minor contribution towards top of the field.

Tuning the IEM

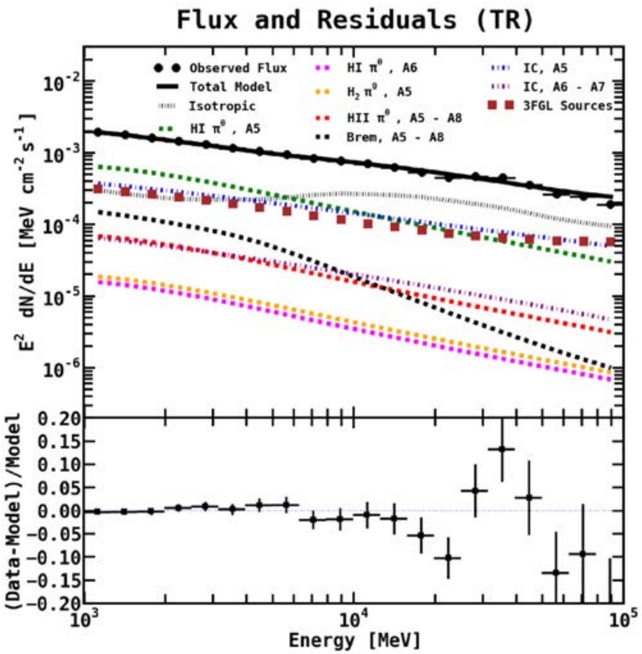

Table 3
Baseline Values for the IEM Components in the TR

Component	Normalization	Flux ($\times 10^{-9}$) (ph cm^{-2} s^{-1})	Intensity ($\times 10^{-8}$) (ph cm^{-2} s^{-1} sr^{-1})
H I π^0, A5	1.10 ± 0.03	439.4 ± 11.0	153.1 ± 3.8
H I π^0, A6	5.0 ± 1.3	10.6 ± 2.8	3.7 ± 1.0
H_2 π^0, A5	2.1 ± 0.1	12.6 ± 0.7	4.4 ± 0.3
Bremsstrahlung	1.0 ± 0.6	100.4 ± 58.3	35.0 ± 20.3
IC, A5	2.3 ± 0.1	274.7 ± 14.0	95.7 ± 4.9
IC, A6 – A7	3.5 ± 0.4	45.7 ± 4.8	15.9 ± 1.7
Isotropic	1.06 ± 0.04	248.1 ± 10.4	86.4 ± 3.6

Note. — The normalizations of the diffuse components are freely scaled, as well as all 3FGL sources in the region. The fit uses the all-sky isotropic spectrum. Intensities are calculated by using the total area of the TR, which is 0.287 sr.

Results for the TR:

- Diffuse components listed in the table are scaled in the fit.
- **Isotropic possesses a normalization of 1.06 +/- 0.04**, which remains fixed for all fits in FM31.
- **Bremsstrahlung possesses a normalization of 1.0 +/- 0.6**, which also remains fixed for all fits in FM31.
- 3FGL sources in the TR are also scaled in the fit, but they do not significantly impact the normalizations of the diffuse components.
- **The model describes the data well across all energies and over the entire region**.
- Residuals worsen at higher energies, but still consistent with statistical fluctuations. Possibly related to poorly modeled 3FGL spectra. We note that it's also possible that the IEM may be compensating for an un-modeled component, i.e. a MW halo component.
- **Normalizations of diffuse components all within reasonable agreement with the GALPROP predictions** (note: IC A6-A7 is a bit high. Same for H I A6, but this component has very little contribution in the TR).

Results for Baseline Fit in FM31

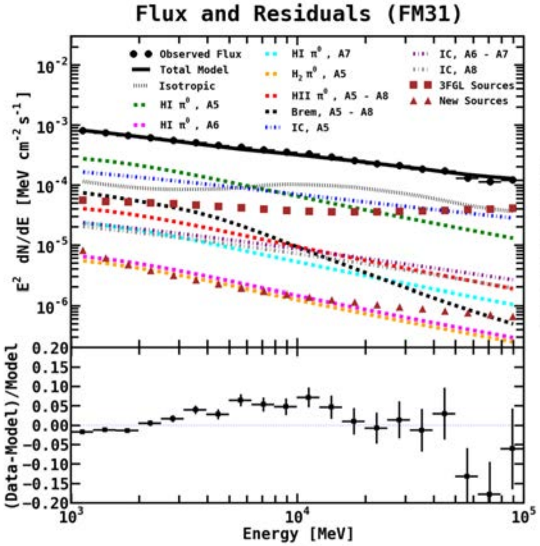

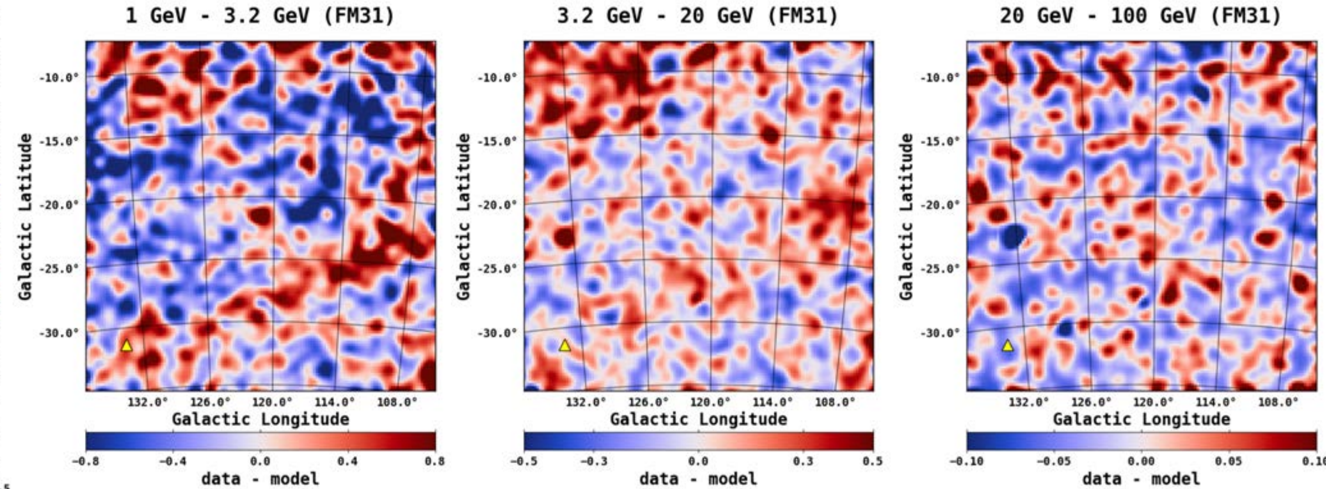

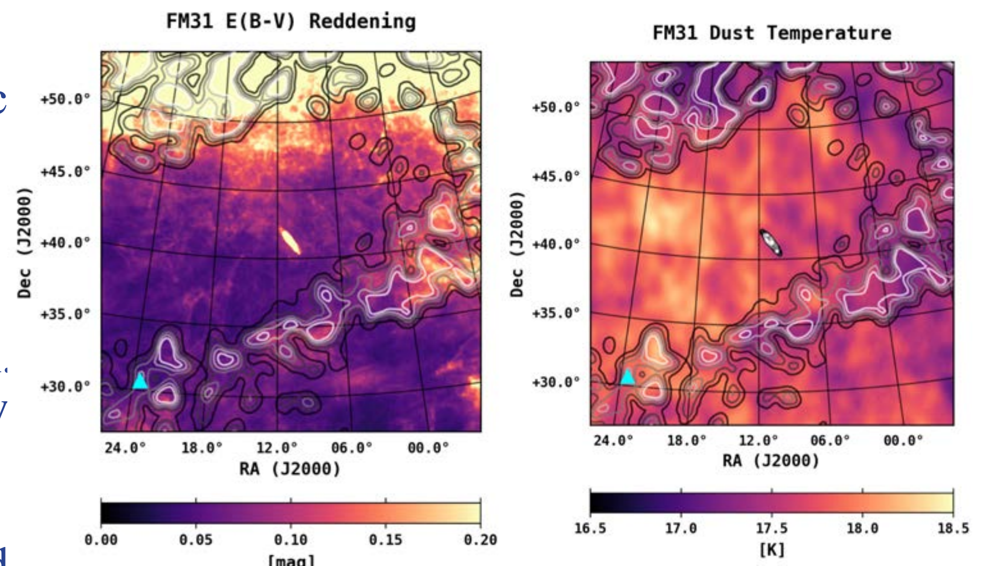

Results for the Baseline Fit in FM31:

- Fit is performed by scaling the diffuse sourc and point sources self-consistently
- **Positive residual emission observed between ~3-20 GeV at the level of ~5%**
- **Spatial residuals show structured excess and deficits**, primarily in the 1st energy bin. Residuals in the 2nd bin are more uniformly distributed, although structures can still be seen.
- The structured emission is likely gas-related (see dust maps)

Results for the Baseline Fit with the Arc Template

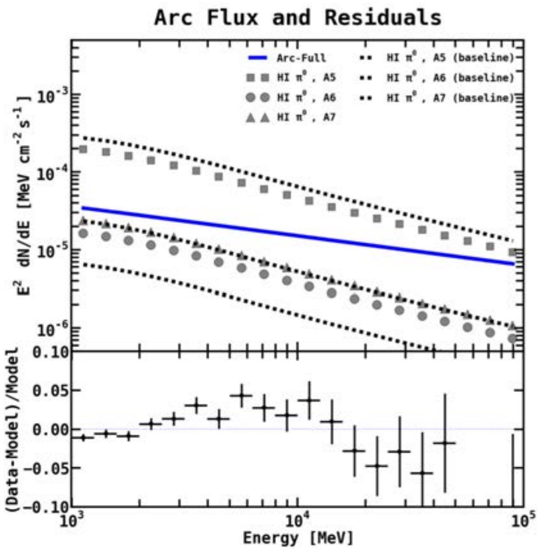

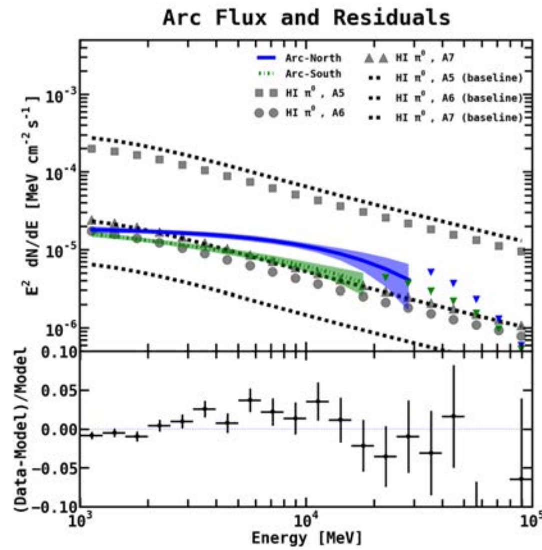

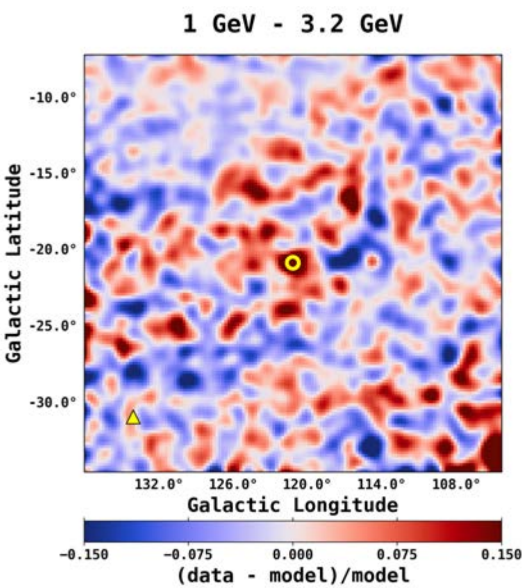

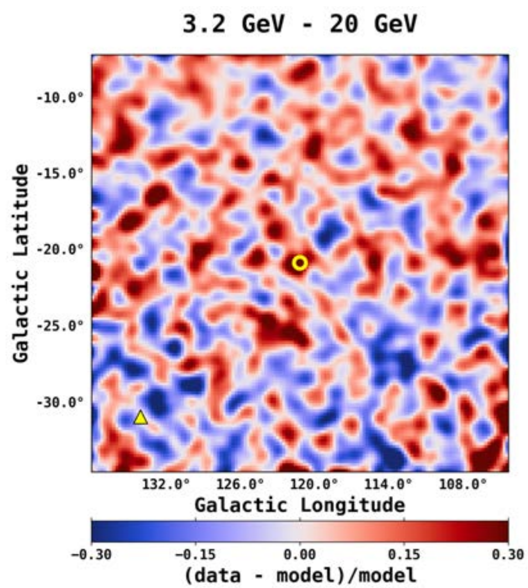

Results for the Arc Fit:

- The arc is fit simultaneously with the other components
- **The arc fit is unable to flatten the positive residual emission between ~3-20 GeV**
- **The index of the arc emission has a value ~2.0-2.4,** notably flatter than the other gas-related emission in the field.
- **The arc emission is found to have a high-energy cutoff**
- The positive residual emission in the second energy bin, associated with the excess between ~3-20 GeV, appears **roughly** uniformly distributed over the field

Interpretation: M31-Related Components

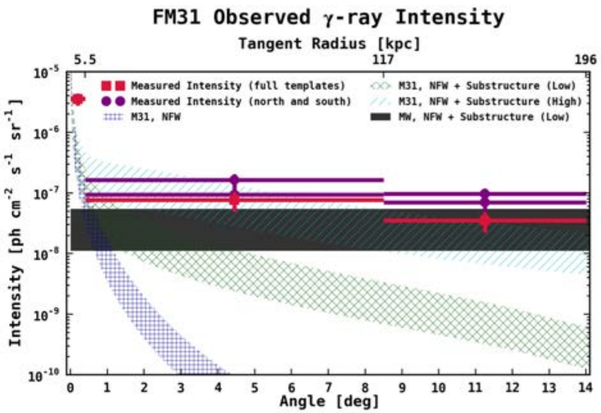

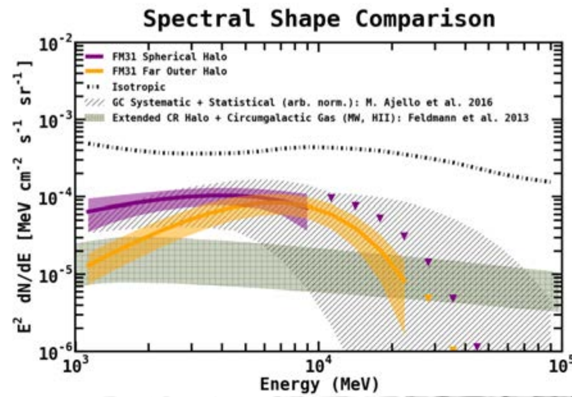

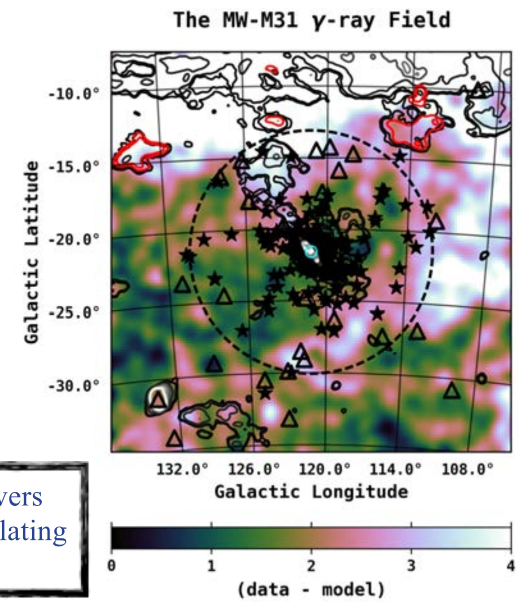

Legend for far right image: solid cyan circle: IG boundary; dashed black circle: SH boundary (FOH covers rest of the field); triangles: M31's dwarfs; stars: M31's globular clusters; contours show H I emission, relating to M33, Wright's cloud, the M31 cloud, cloud of Complex H (shown in red), and the MW plane (top).

- ◇ **We compare the observed excess with (simplified) predictions for a DM signal that originates from the M31 halo, with a spectrum and annihilation cross-section consistent with a DM interpretation of the GC excess.**
- ◇ We consider the contribution from both the M31 halo and the MW halo along the line of sight, since the MW component has not been explicitly accounted for in our analysis, and may be at least partially embedded within the isotropic component and other IEM components.
- ◇ We consider different assumptions for the amount of DM substructure in M31 (and the MW), and **we find that if a cold DM scenario is assumed that includes a large boost factor due to substructures, the observed excess emission is consistent with this interpretation.**
- ◇ The spherical halo component is found to enclose 68% (19/28) of M31's dwarf galaxy population, which increases to 82% (23/28) if including the dwarfs which are within ~1 degree of the spherical halo boundary.

The excess in different foreground models

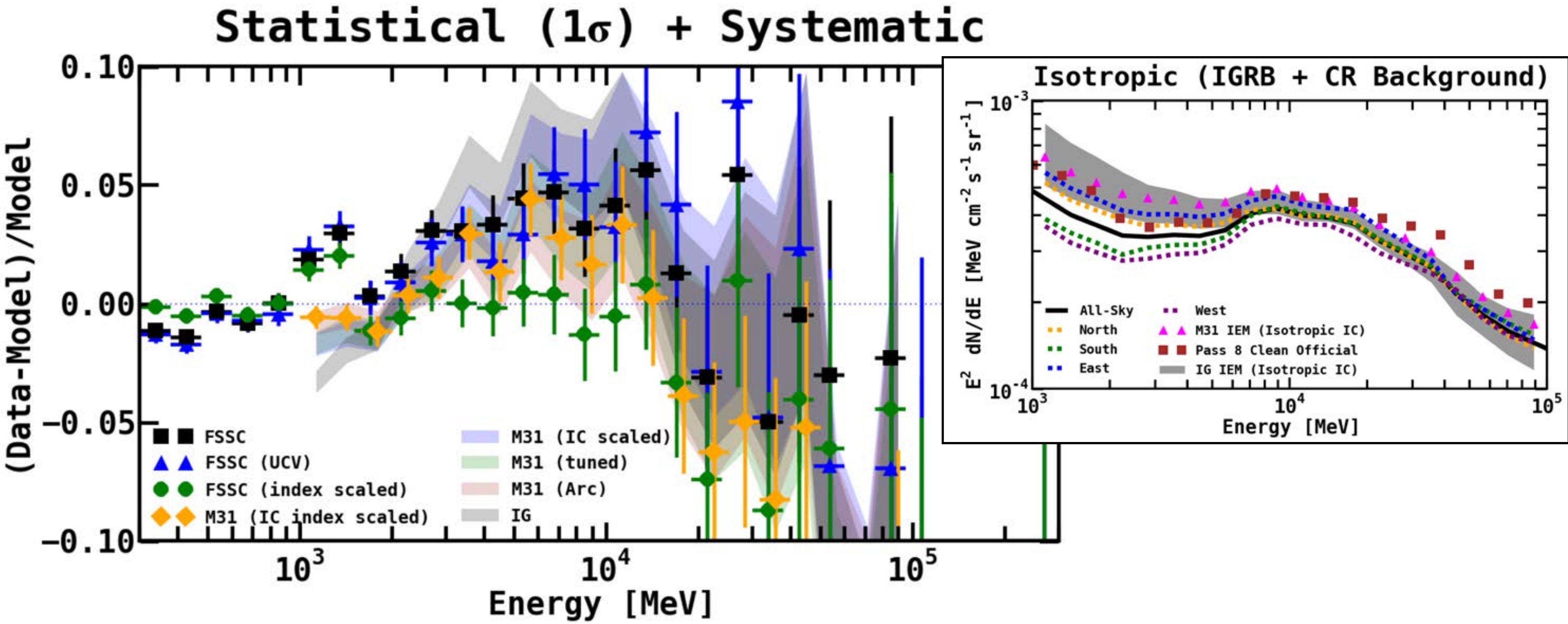

The green data points result from using the FSSC IEM, scaling all the parameters (including the index), and fitting all components in the signal region (including the isotropic). **Black squares:** FSSC IEM: scaling the isotropic and Galactic (with index fixed) in the signal region, using Clean data. **Blue triangles:** FSSC IEM (UCV): same as above but using UltraCleanVeto (UCV) data. **Dark yellow diamonds:** M31 IC index scaled (fit). The index scaling mostly affects outer Galaxy IC A6-A8. **Blue band:** M31 IC scaled: baseline fit using M31 IEM with IC scaled corresponding to Figure 18 in draft. **Green band:** M31 (tuned): tuned baseline fit using M31 IEM corresponding to Figure 14 in draft. **Pink band:** M31 (Arc): arc fit with M31 IEM corresponding to Figure 22 in draft. **Black band:** IG: baseline fit with the inner Galaxy (IG) IEM corresponding to Figure B2 in draft. All bands give 1 sigma error.

In place of a conclusion

In respect of CR with $E_{CR}<10^{15}\div10^{16}$ eV there generally remain some vague points, but on the whole the picture is clear enough…

— V.L. Ginzburg, 1999

There is nothing new to be discovered in physics now. All that remains is more and more precise measurement

— Lord Kelvin, 1900